

Time-Sliced Perturbation Theory for Large Scale Structure I: General Formalism

Diego Blas,^{a,1} Mathias Garny,^{a,2} Mikhail M. Ivanov^{b,c,d,3} and Sergey Sibiryakov,^{a,b,d,4}

^a*CERN Theory Division, CH-1211 Genève 23, Switzerland*

^b*FSB/ITP/LPPC, École Polytechnique Fédérale de Lausanne, CH-1015, Lausanne, Switzerland*

^c*Faculty of Physics, Moscow State University, Vorobjevy Gory, 119991 Moscow, Russia*

^d*Institute for Nuclear Research of the Russian Academy of Sciences,
60th October Anniversary Prospect, 7a, 117312 Moscow, Russia*

ABSTRACT: We present a new analytic approach to describe large scale structure formation in the mildly non-linear regime. The central object of the method is the time-dependent probability distribution function generating correlators of the cosmological observables at a given moment of time. Expanding the distribution function around the Gaussian weight we formulate a perturbative technique to calculate non-linear corrections to cosmological correlators, similar to the diagrammatic expansion in a three-dimensional Euclidean quantum field theory, with time playing the role of an external parameter. For the physically relevant case of cold dark matter in an Einstein–de Sitter universe, the time evolution of the distribution function can be found exactly and is encapsulated by a time-dependent coupling constant controlling the perturbative expansion. We show that all building blocks of the expansion are free from spurious infrared enhanced contributions that plague the standard cosmological perturbation theory. This paves the way towards the systematic resummation of infrared effects in large scale structure formation. We also argue that the approach proposed here provides a natural framework to account for the influence of short-scale dynamics on larger scales along the lines of effective field theory.

¹diego.blas@cern.ch

²mathias.garny@cern.ch

³mikhail.ivanov@cern.ch

⁴sergey.sibiryakov@cern.ch

Contents

1	Introduction	1
2	Perfect fluid evolution equations	4
3	The TSPT framework	5
3.1	Preliminaries	5
3.2	Vertices	7
3.3	Perturbative expansion	10
3.4	More than one field	12
4	Application to Zel’dovich approximation and exact dynamics	14
4.1	Zel’dovich approximation	14
4.1.1	The density field	15
4.2	Exact dynamics	16
5	Soft limits and infrared safety	17
5.1	Vertices with soft momenta	17
5.2	Relation to the equivalence principle	19
6	Discussion	21
A	TSPT kernels from SPT	23
B	1-loop results and comparison with SPT	23
C	IR safety and the initial power spectrum	25

1 Introduction

Ongoing and future cosmological surveys will provide an unprecedented amount of data about the structure of the universe at large scales. The statistical properties of this large scale structure (LSS) are believed to contain a wealth of information about the primordial constituents and dynamical evolution of the universe. However, harvesting this information will not be an easy task and will require, in particular, a precise theoretical understanding of self-gravitating systems far away from equilibrium. The most straightforward approach to this problem relies on current computer power to produce realistic N -body simulations for a large range of scales. Impressive as they are, these simulations are still very time-consuming, which calls for (semi-)analytic methods. At the largest scales, above *a few* megaparsecs, the dynamics is dominated by dark matter which, in turn, can be described

as an almost perfect pressureless fluid, possibly with stochastic sources [1–6]. At these scales the matter density contrast is a small quantity which justifies the use of perturbative techniques.

Standard perturbation theory (SPT) of LSS formation [7, 8] is one of the most popular of these techniques. It consists of two main steps: first, one expresses the dark matter density- and velocity fields at a given time as a power series of the initial conditions, assuming a perfect pressureless fluid without vorticity. Next, one performs the ensemble averages using the statistical distribution at the initial time when the system is well within the linear regime. The initial distribution is often taken to be Gaussian¹, as motivated by the constraints coming from the cosmic microwave background measurements [9]. This framework leads to a loop expansion for non-linear corrections to cosmological correlation functions and has provided numerous insights into their properties.

However, SPT possesses a number of drawbacks which have recently attracted significant attention. They can be attributed to the sensitivity of the SPT computational scheme to the infrared (IR) and ultraviolet (UV) modes. The presence of mode-mixing is a consequence of the non-linear dynamics. In the loop integrals of SPT this effect receives large contributions both from very small (IR) and very large (UV) wavenumbers. Technically, the individual loop integrals in SPT would be IR (UV) divergent for an initial power spectrum² $P(k)$ behaving as k^ν with $\nu \leq -1$ ($\nu > -3$) at $k \rightarrow 0$ ($k \rightarrow \infty$)³. Realistic Λ CDM spectra avoid these conditions and divergences are absent. However, the corresponding IR/UV regions in the loop integrals still give rise to large contributions that ultimately limit the applicability of perturbative computations. They are somewhat loosely referred to as “IR/UV divergences” even for Λ CDM.

Qualitatively the appearance of IR divergences in SPT stems from the use of the initial distribution to evaluate quantities at late times. This introduces non-local time dependence to the large displacements of the fluid particles caused by large scale bulk flows. It is well known that the IR divergences cancel out in equal-time correlators upon summing over all sub-diagrams at a fixed order in perturbation theory [11]. This cancellation has been formally proven for *leading* IR divergences to all orders of perturbation theory [12] and can be traced back to the equivalence principle [13, 14]. Recently, the cancellation has been proven also for *subleading* IR divergences showing up for the first time at 2 loops [15–19]. Still, the presence of spurious IR divergences greatly complicates numerical calculations⁴ and obscures the analysis of physical effects produced by the large scale bulk flows. The latter, though finite, have a strong impact on the features in the cosmological correlation functions [21]. In particular, a resummation of physical IR contributions is essential for an accurate description of baryon acoustic oscillations (BAO) in the power spectrum [21–24].

¹It is worth stressing that the precise form of the distribution should be provided by the theory describing the generation of primordial fluctuations. Disentangling the primordial non-Gaussianity from the secondary one induced by non-linear dynamics constitutes one of the goals of the LSS studies.

²We refer as ‘initial’ to quantities defined after recombination, that serve as the input for non-linear structure formation.

³More precisely, UV divergences arise at L -loop order if $\nu \geq -3 + 2/L$ for $k \rightarrow \infty$ [10].

⁴IR-safe integrands have been constructed in [15, 16] for 2 loops and in [20] for an arbitrary L -loop order.

Another problem is related to the UV sensitivity of the SPT loop expansion [8, 20]. This makes the perturbative results at high loop order largely dependent on the short wavelength modes. In particular, the calculations are very sensitive to the scales where the fluid approach fails. This issue was recently addressed by applying ideas of effective theories to LSS [5]. In these approaches, one renormalizes the UV contributions and parameterizes the ignorance about the dynamics at short scales by various effective operators in the equations of motion of the dark matter fluid which are fixed from data or N -body simulations, see [25, 26]. They exhibit non-local time dependence, which complicates the renormalisation at high loop order [27]. Yet, the results from N -body simulations show that the actual sensitivity of the power spectrum to UV modes is smaller than what is observed in SPT [2, 28, 29], confirming the expectations based on qualitative arguments [1]. This suggests that an accurate description of LSS based on perturbation theory may be possible under rather broad assumptions about the short-scale dynamics. Therefore, one is motivated to develop approaches where the UV contributions can be consistently isolated and their sensitivity to various assumptions systematically studied [4, 30, 31].

In this paper, we advocate a new framework within Eulerian hydrodynamics which can overcome the aforementioned drawbacks of SPT. The main idea is to evolve the statistical distribution function of the fields rather than the fields themselves. This is done using the Liouville equation of statistical mechanics. The perturbation theory is then developed over the Gaussian part of the distribution at final time. The latter closely resembles perturbation theory in a (non-local) 3-dimensional Euclidean quantum field theory (QFT), with time playing the role of an external parameter⁵. In this way, we disentangle time evolution from statistical averaging. We denote the formalism by *Time-Sliced Perturbation Theory* (TSPT). We are going to argue that it is well adapted for calculating cosmological correlators with all entries taken at the same time. These observables are of particular interest in cosmological observations [7].

The strategy to evolve the distribution function can in principle be applied to any underlying evolution equations, and we pay special attention to keep the derivation general. For the equations of a pressureless perfect fluid and at a fixed order of perturbation theory the TSPT approach gives the same results as SPT. Nonetheless, we will show that TSPT has the important advantage that all building blocks of the diagrammatic expansion, i.e. propagators and vertices, as well as individual diagrams themselves are free from IR divergences. This can be traced back to the property that within TSPT one deals only with equal-time objects which are protected from spurious divergences by the equivalence principle. TSPT is thus a convenient framework for implementing IR resummation — a subject that is addressed in [32]. On the UV side, TSPT allows to reformulate the effective field theory of LSS in the language of Wilsonian renormalization group within the 3-dimensional Euclidean QFT describing the statistical averaging. This formulation appears promising to shed new light on the properties of the effective operators. The inclusion of stochastic noise in the evolution [5, 6] can, in principle, be incorporated by promoting the Liouville

⁵We will see that for Einstein–de Sitter cosmology time enters through a time-dependent coupling constant controlling the perturbative expansion. This is also a very good approximation in the Λ CDM case.

equation for the distribution function to a Fokker-Planck equation. Finally, the structure of TSPT is also suitable to include primordial non-Gaussianity in a straightforward manner.

The paper is organized as follows. In sec. 2 we recall the Eulerian fluid equations, define the Zel'dovich approximation and fix our notations. The general formalism is introduced in sec. 3, where we present the strategy to solve the Liouville equation and derive the perturbative expansion for correlation functions. We apply this method to the Zel'dovich approximation in sec. 4.1 and to the exact Eulerian dynamics in sec. 4.2. In sec. 5 we prove the IR finiteness of the vertex functions and relate it to the equivalence principle. Section 6 is devoted to discussion and future directions. Formulas relating the TSPT vertex functions with the SPT kernels are given in appendix A. Appendix B contains an explicit example of a one-loop computation in TSPT and its comparison to the SPT result. Finally, appendix C is devoted to some technical details regarding the IR - safety of TSPT vertices.

2 Perfect fluid evolution equations

In this section we fix our notations and conventions by briefly reminding the basic equations underlying the SPT approach (see [7, 8] for a detailed discussion). In general, the evolution of non-relativistic, gravitationally interacting matter in an expanding universe is described by the Vlasov–Poisson equation for the phase-space distribution function. By taking moments of the distribution function over the velocity one obtains a coupled hierarchy of evolution equations. Its truncation leads to the Eulerian equations for a perfect pressureless fluid,

$$\frac{\partial \delta}{\partial t} + \nabla \cdot [(1 + \delta)\mathbf{u}] = 0, \quad (2.1a)$$

$$\frac{\partial \mathbf{u}}{\partial t} + \mathcal{H}\mathbf{u} + (\mathbf{u} \cdot \nabla)\mathbf{u} = -\nabla\Phi, \quad (2.1b)$$

where t is the conformal time, $\delta(t, \mathbf{x})$ is the overdensity field and $\mathbf{u}(t, \mathbf{x})$ is the peculiar flow velocity. The gravitational potential is determined by the Poisson equation

$$\nabla^2\Phi = \frac{3}{2}\mathcal{H}^2\Omega_m\delta, \quad (2.1c)$$

where $\mathcal{H} = aH$ is the conformal Hubble rate, and Ω_m is the time-dependent matter density parameter. It is convenient to introduce a new time variable

$$\eta \equiv \log D_+(t),$$

where $D_+(t)$ is the growth factor of the linearized perturbations, and rewrite eqs. (2.1) in Fourier space. Neglecting vorticity, which decays at the linear level and is not sourced by the gradient force, we obtain,

$$\dot{\delta}_\eta(\mathbf{k}) - \Theta_\eta(\mathbf{k}) = \int [dq]^2 \delta^{(3)}(\mathbf{k} - \mathbf{q}_1 - \mathbf{q}_2) \alpha(\mathbf{q}_1, \mathbf{q}_2) \Theta_\eta(\mathbf{q}_1) \delta_\eta(\mathbf{q}_2), \quad (2.2a)$$

$$\dot{\Theta}_\eta(\mathbf{k}) - \frac{3\Omega_m}{2f^2} \delta_\eta(\mathbf{k}) + \left(\frac{3\Omega_m}{2f^2} - 1 \right) \Theta_\eta(\mathbf{k}) = \int [dq]^2 \delta^{(3)}(\mathbf{k} - \mathbf{q}_1 - \mathbf{q}_2) \beta(\mathbf{q}_1, \mathbf{q}_2) \Theta_\eta(\mathbf{q}_1) \Theta_\eta(\mathbf{q}_2), \quad (2.2b)$$

where dot stands for a derivative with respect to η , and we have introduced the notations,

$$\delta_\eta(\mathbf{k}) \equiv \delta(\eta, \mathbf{k}) , \quad \Theta_\eta(\mathbf{k}) \equiv -\frac{\nabla \mathbf{u}(\eta, \mathbf{k})}{f(\eta) \mathcal{H}(\eta)} \quad \text{with} \quad f \equiv \frac{d \ln D_+(\eta)}{d \ln a(\eta)} . \quad (2.3)$$

Note that we have rescaled the velocity divergence to minimize the η -dependence in the equations. The non-linear kernels are given by

$$\alpha(\mathbf{k}_1, \mathbf{k}_2) \equiv \frac{(\mathbf{k}_1 + \mathbf{k}_2) \cdot \mathbf{k}_1}{k_1^2} , \quad \beta(\mathbf{k}_1, \mathbf{k}_2) \equiv \frac{(\mathbf{k}_1 + \mathbf{k}_2)^2 (\mathbf{k}_1 \cdot \mathbf{k}_2)}{2k_1^2 k_2^2} . \quad (2.4)$$

Finally, we have used a shorthand notation for the integration measure, $[dq]^n \equiv d^3 q_1 \cdots d^3 q_n$.

In a matter-dominated universe (Einstein–de Sitter background) one has $\Omega_m = f = 1$ and the coefficients in eqs. (2.2) are time-independent. For Λ CDM cosmology the ratio Ω_m/f^2 is also close to one and we will simplify eqs. (2.2) by replacing $\Omega_m/f^2 \mapsto 1$. As shown in [33] (see also [7]), the error in the power spectrum introduced by this replacement is less than 1% at zero redshift ($z = 0$) and less than 0.1% at $z = 1$ for all relevant scales. Thus, this replacement provides an accurate approximation to the exact dynamics and the deviation of Ω_m/f^2 from 1 can be taken into account perturbatively. With slight abuse of language we refer to the case described by eqs. (2.2) with $\Omega_m/f^2 = 1$ as “exact dynamics” (ED).

Below we also consider the Zel’dovich approximation (ZA) which is obtained by replacing δ in (2.2b) with Θ . In this case (2.2b) becomes a closed equation for Θ . While in ZA the correlation functions of cosmological observables can be found exactly, for us it is relevant as a testing ground of our perturbative technique. ZA also captures correctly the effects of large bulk flows in ED and hence both approaches share a similar IR behavior [13]. However, one should keep in mind that in all other regimes the properties of ZA and ED are essentially different.

3 The TSPT framework

3.1 Preliminaries

In this section we develop the TSPT formulation for general evolution equations, irrespectively of particular approximations for the fluid dynamics. We start by considering a single field variable, which, to avoid proliferation of notations, we denote with the same letter Θ as the velocity divergence. It satisfies the deterministic equation of motion,

$$\dot{\Theta}_\eta(\mathbf{k}) = \mathcal{I}[\Theta_\eta; \eta, \mathbf{k}] , \quad (3.1)$$

where the r.h.s. is given as a Taylor series in the fields,

$$\mathcal{I}[\Theta_\eta; \eta, \mathbf{k}] = \sum_{n=1}^{\infty} \frac{1}{n!} \int [dq]^n I_n(\eta; \mathbf{q}_1, \dots, \mathbf{q}_n) \delta^{(3)}\left(\mathbf{k} - \sum_{i=1}^n \mathbf{q}_i\right) \prod_{j=1}^n \Theta_\eta(\mathbf{q}_j) . \quad (3.2)$$

The δ -function in this expression enforces the conservation of momentum, which we assume to be satisfied by the system. We also assume that the system respects parity

$$I_m(\eta; \mathbf{q}_1, \dots, \mathbf{q}_m) = I_m(\eta; -\mathbf{q}_1, \dots, -\mathbf{q}_m) . \quad (3.3)$$

The second key ingredient is the statistical distribution at the initial time η_0 chosen deep in the linear regime. For illustrative purposes, let us assume that it is Gaussian. This is a very good approximation for LSS, consistent with the Planck results [9]. We will discuss how to include an initial non-Gaussianity later on. According to this assumption, the correlators of Θ_η are determined by the generating functional [34, 35],

$$Z[J; \eta] = \mathcal{N}^{-1} \int [\mathcal{D}\Theta_{\eta_0}] \exp \left\{ -\frac{1}{2} \int [dk] \frac{\Theta_{\eta_0}(\mathbf{k}) \Theta_{\eta_0}(-\mathbf{k})}{P_{\eta_0}(|\mathbf{k}|)} + \int [dk] \Theta_\eta(\mathbf{k}) J(-\mathbf{k}) \right\}, \quad (3.4)$$

where

$$\mathcal{N} = \int [\mathcal{D}\Theta_{\eta_0}] \exp \left\{ -\frac{1}{2} \int [dk] \frac{\Theta_{\eta_0}(\mathbf{k}) \Theta_{\eta_0}(-\mathbf{k})}{P_{\eta_0}(|\mathbf{k}|)} \right\}, \quad (3.5)$$

is the normalization factor. Note that the integration here is performed over the fields at the initial time, whereas the source J couples to the final values of the field. We have explicitly implemented the statistical homogeneity and isotropy by postulating that in the Gaussian weight the momenta of the Θ -fields sum to zero and the power spectrum $P_{\eta_0}(|\mathbf{k}|)$ depends only on the absolute value of the momentum. The equal-time correlation functions are obtained by varying $Z[J; \eta]$ with respect to the source and setting $J = 0$ afterwards,

$$\langle \Theta_\eta(\mathbf{k}_1) \dots \Theta_\eta(\mathbf{k}_n) \rangle = \frac{\delta^n Z[J; \eta]}{\delta J(-\mathbf{k}_1) \dots \delta J(-\mathbf{k}_n)} \Big|_{J=0}. \quad (3.6)$$

In particular, for the two-point function at the initial time this formula yields,

$$\langle \Theta_{\eta_0}(\mathbf{k}_1) \Theta_{\eta_0}(\mathbf{k}_2) \rangle = \frac{\delta^2 Z[J; \eta_0]}{\delta J(-\mathbf{k}_1) \delta J(-\mathbf{k}_2)} \Big|_{J=0} = P_{\eta_0}(|\mathbf{k}_1|) \delta^{(3)}(\mathbf{k}_1 + \mathbf{k}_2). \quad (3.7)$$

In SPT the evolution equations (3.1) are solved iteratively and the final field $\Theta_\eta(\mathbf{k})$ is expressed as a Taylor series in the powers of the initial configuration $\Theta_{\eta_0}(k)$, see eq. (A.1) in appendix A. We suggest an alternative procedure. If one is only interested in correlation functions of fields at a particular time, it seems natural to use them as the main elements of the analysis. To do this, we substitute the integration variable in (3.4) by the fields at time η , which defines a time-dependent distribution function $\mathcal{P}[\Theta_\eta; \eta]$,

$$Z[J; \eta] = \int [\mathcal{D}\Theta_\eta] \mathcal{P}[\Theta_\eta; \eta] \exp \left\{ \int [dk] \Theta_\eta(\mathbf{k}) J(-\mathbf{k}) \right\}. \quad (3.8)$$

The equation that determines the time evolution of \mathcal{P} is nothing but the classical *Liouville* equation where the value of the field at a particular \mathbf{k} is considered as a statistical variable. For a system obeying (3.1) it reads,

$$\frac{\partial}{\partial \eta} \mathcal{P}[\Theta_\eta; \eta] + \int [dk] \frac{\delta}{\delta \Theta_\eta(\mathbf{k})} \left(\mathcal{I}[\Theta_\eta; \eta, \mathbf{k}] \mathcal{P}[\Theta_\eta; \eta] \right) = 0. \quad (3.9)$$

This equation can be understood as the continuity equation for the probability density in functional space. It can be derived by performing a substitution of integration variables in (3.8) in terms of fields at time $\eta + \delta\eta$, and taking $\delta\eta \rightarrow 0$ while demanding the invariance of generating functional on the choice of integration variables. In what follows, we derive a

recursive chain of equations to solve (3.9). When \mathcal{P} is found, one can compute the different correlation functions using (3.8). In this way we disentangle the time evolution from the statistical averaging. From now on we will omit the subindex “ η ” on the field Θ whenever it appears as the argument of the distribution function.

3.2 Vertices

We search for the solution of (3.8) in the form,

$$\mathcal{P}[\Theta; \eta] = \mathcal{N}^{-1} \exp \{ -\Gamma[\Theta; \eta] \}. \quad (3.10)$$

In the spirit of perturbation theory, we expand the statistical weight Γ as a series in the powers of the field Θ ,

$$\Gamma[\Theta; \eta] = \sum_{n=1}^{\infty} \frac{1}{n!} \int [dk]^n \Gamma_n^{tot}(\eta; \mathbf{k}_1, \dots, \mathbf{k}_n) \prod_{j=1}^n \Theta(\mathbf{k}_j). \quad (3.11)$$

Substituting this into (3.9), using the expression (3.2) and requiring that the coefficients in front of equal powers of Θ vanish we obtain,

$$\begin{aligned} \dot{\Gamma}_n^{tot}(\eta; \mathbf{k}_1, \dots, \mathbf{k}_n) &+ \sum_{m=1}^n \frac{1}{m!(n-m)!} \\ &\times \sum_{\sigma} I_m(\eta; \mathbf{k}_{\sigma(1)}, \dots, \mathbf{k}_{\sigma(m)}) \Gamma_{n-m+1}^{tot} \left(\eta; \sum_{l=1}^m \mathbf{k}_{\sigma(l)}, \mathbf{k}_{\sigma(m+1)}, \dots, \mathbf{k}_{\sigma(n)} \right) \\ &= \delta^{(3)} \left(\sum_{i=1}^n \mathbf{k}_i \right) \int [dp] I_{n+1}(\eta; \mathbf{p}, \mathbf{k}_1, \dots, \mathbf{k}_n), \end{aligned} \quad (3.12)$$

where in the second term on the l.h.s. the sum runs over all permutations σ of n indices. Note that, by construction, I_n, Γ_n^{tot} are symmetric functions of momenta, and thus the terms obtained by permutations inside the first m or last $(n-m)$ momenta are the same. In other words, the number of distinct terms in the sum over σ is equal to the binomial coefficient $\binom{n}{m}$ instead of $n!$. The chain of equations (3.12) can be compared to the so-called BBGKY hierarchy for the correlation functions appearing in the standard approach [1]. A key difference is that in our case the n -th equation contains only the functions Γ_m^{tot} with $m \leq n$ and hence can be solved exactly. In contrast, in the BBGKY hierarchy the equation for the n -point function involves higher correlators. To solve it, one has to truncate the hierarchy at a finite order, thereby introducing an error in the solution. Still, the approach can be useful to solve SPT perturbatively [36].

We will see in sec. 4 that for the evolution equations describing the dynamics of LSS the momentum integrals appearing on the r.h.s. of eq. (3.12) are UV divergent. Thus, it is convenient to split Γ_n^{tot} into a regular part Γ_n and a singular ‘counterterm’ C_n ,

$$\Gamma_n^{tot} = \Gamma_n + C_n. \quad (3.13)$$

The vertex functions Γ_n satisfy (3.12) without sources and are subject to initial conditions encoding the statistical properties of the primordial fluctuations. The C_n satisfy trivial

initial conditions and are sourced by the divergent r.h.s. in (3.12). As we will discuss shortly, they cancel certain UV divergent contributions in the diagrammatic expansion based on (3.8), hence the name ‘counterterms’. The divergences stem from the (singular) Jacobian describing the change in the functional measure when going from (3.4) to (3.8).

To proceed, let us assume that the evolution kernels I_n are time-independent. As discussed in sec. 2, this is a good approximation in the case of LSS. We further take

$$I_1 = 1 , \quad (3.14)$$

which implies that the solution of linearized evolution equations (3.1) grows as e^η uniformly at all momenta. This is the case for a perfect pressureless fluid.⁶ Let us first focus on the regular vertices Γ_n . It is easy to see that Γ_1 can be consistently set to 0 at all times, which corresponds to vanishing one-point function $\langle \Theta_\eta \rangle = 0$. For $n \geq 2$ we use the Ansatz,

$$\Gamma_n(\eta; \mathbf{k}_1, \dots, \mathbf{k}_n) = \sum_{l=2}^n e^{-l\eta} \Gamma_n^{(l)}(\mathbf{k}_1, \dots, \mathbf{k}_n) . \quad (3.15)$$

Substituting it into (3.12) with vanishing r.h.s. yields a chain of relations,

$$\begin{aligned} \Gamma_n^{(l)}(\mathbf{k}_1, \dots, \mathbf{k}_n) &= -\frac{1}{n-l} \sum_{m=2}^{n-l+1} \frac{1}{m!(n-m)!} \\ &\times \sum_{\sigma} I_m(\mathbf{k}_{\sigma(1)}, \dots, \mathbf{k}_{\sigma(m)}) \Gamma_{n-m+1}^{(l)}\left(\sum_{i=1}^m \mathbf{k}_{\sigma(i)}, \mathbf{k}_{\sigma(m+1)}, \dots, \mathbf{k}_{\sigma(n)}\right), \end{aligned} \quad (3.16)$$

for $2 \leq l < n$, whereas $\Gamma_n^{(n)}$ is arbitrary. The latter must be determined by the initial conditions on Γ_n . To simplify the formulas, it is convenient to send the initial time η_0 to $-\infty$. We obtain,

$$\Gamma_n^{(n)}(\mathbf{k}_1, \dots, \mathbf{k}_n) = \lim_{\eta_0 \rightarrow -\infty} e^{n\eta_0} \Gamma_n(\eta_0; \mathbf{k}_1, \dots, \mathbf{k}_n) . \quad (3.17)$$

The solution (3.15) is greatly simplified in the physically relevant case of Gaussian initial conditions. According to (3.17) the initial data in this case read,

$$\Gamma_2^{(2)}(\mathbf{k}_1, \mathbf{k}_2) = \frac{\delta^{(3)}(\mathbf{k}_1 + \mathbf{k}_2)}{\bar{P}(|\mathbf{k}_1|)} , \quad (3.18a)$$

$$\Gamma_n^{(n)} = 0 , \quad n > 2 . \quad (3.18b)$$

Here

$$\bar{P}(|\mathbf{k}|) \equiv \lim_{\eta_0 \rightarrow -\infty} e^{-2\eta_0} P_{\eta_0}(|\mathbf{k}|) \quad (3.19)$$

⁶A momentum dependence of the growth factor appears beyond the perfect fluid approximation [3, 30].

is the suitably rescaled initial power spectrum. Next, from (3.16) one infers that all $\Gamma_n^{(l)}$ with $l > 2$ vanish, which leads to the solution

$$\Gamma_n(\eta; \mathbf{k}_1, \dots, \mathbf{k}_n) = e^{-2\eta} \bar{\Gamma}_n(\mathbf{k}_1, \dots, \mathbf{k}_n), \quad (3.20a)$$

$$\begin{aligned} \bar{\Gamma}_n(\mathbf{k}_1, \dots, \mathbf{k}_n) = & -\frac{1}{n-2} \sum_{m=2}^{n-1} \frac{1}{m!(n-m)!} \\ & \times \sum_{\sigma} I_m(\mathbf{k}_{\sigma(1)}, \dots, \mathbf{k}_{\sigma(m)}) \bar{\Gamma}_{n-m+1} \left(\sum_{i=1}^m \mathbf{k}_{\sigma(i)}, \mathbf{k}_{\sigma(m+1)}, \dots, \mathbf{k}_{\sigma(n)} \right), \end{aligned} \quad (3.20b)$$

where we have introduced the notation $\bar{\Gamma}_n \equiv \Gamma_n^{(2)}$. One observes that all vertices are proportional to the same factor $e^{-2\eta}$. This implies that the time dependence factors out of the regular part of statistical weight⁷ (3.11). It is suggestive to write it in the form,

$$\Gamma^{reg}[\Theta; \eta] = \frac{1}{g^2(\eta)} \bar{\Gamma}[\Theta], \quad (3.21)$$

where

$$g(\eta) \equiv e^{\eta} \quad (3.22)$$

and $\bar{\Gamma}[\Theta]$ is time-independent. This expression implies that g plays the role of the *coupling constant* controlling the perturbative expansion of the generating functional (3.8). Note that g grows with time, so that the perturbation theory breaks down at late times, as expected for the dynamics of gravitational clustering. Practical computations up to a fixed order in perturbative expansion require the knowledge of only a few lowest-order vertices. These can be easily found from the recursion relations (3.20b) with the seed two-point function $\bar{\Gamma}_2$ given by (3.18a). Explicit expressions for the three- and four-point vertices are given in appendix B.

It is clear how to include initial non-Gaussianity in this framework. For instance, the presence of an initial bispectrum gives rise to non-vanishing vertex $\Gamma_3^{(3)}$. Through eqs. (3.16) this will generate a sequence of descendant contributions in all vertices with $n \geq 4$. Note that these contributions scale with time as $e^{-3\eta}$. Therefore, they decay compared to the higher-point vertices induced by non-linear evolution which scale as $e^{-2\eta}$. For the sake of the presentation, we will focus on the Gaussian case in the rest of the paper.

We now turn to the counterterms C_n . From eq. (3.12) and in the limit $\eta_0 \rightarrow -\infty$ they are found to be time-independent and determined by the recursion relations,

$$\begin{aligned} C_n(\mathbf{k}_1, \dots, \mathbf{k}_n) = & \frac{1}{n} \left[\delta^{(3)} \left(\sum_{i=1}^n \mathbf{k}_i \right) \int [dq] I_{n+1}(\mathbf{q}, \mathbf{k}_1, \dots, \mathbf{k}_n) \right. \\ & \left. - \sum_{m=2}^n \frac{1}{m!(n-m)!} \sum_{\sigma} I_m(\mathbf{k}_{\sigma(1)}, \dots, \mathbf{k}_{\sigma(m)}) C_{n-m+1} \left(\sum_{l=1}^m \mathbf{k}_{\sigma(l)}, \mathbf{k}_{\sigma(m+1)}, \dots, \mathbf{k}_{\sigma(n)} \right) \right], \end{aligned} \quad (3.23)$$

⁷The time-dependence of the counterterms C_n is different, see eq. (3.23).

where⁸ $n \geq 1$ and for $n = 1$ the sum should be omitted. Comparing this with the “tree-level” weight (3.21) we see that the counterterms are suppressed by the second power of the coupling constant $g(\eta)$. This is precisely the suppression expected for 1-loop contributions. Indeed, we will see that C_n cancel certain UV divergences of the 1-loop expressions.

Finally, statistical homogeneity implies that all the vertices and counterterms are proportional to a δ -function of the sum of the momenta entering them. We will use prime to denote the quantities stripped of this δ -function, as has become customary in the studies of LSS,

$$\bar{\Gamma}_n = \bar{\Gamma}'_n(\mathbf{k}_1, \dots, \mathbf{k}_n) \delta^{(3)}\left(\sum_{i=1}^n \mathbf{k}_i\right), \quad C_n = C'_n(\mathbf{k}_1, \dots, \mathbf{k}_n) \delta^{(3)}\left(\sum_{i=1}^n \mathbf{k}_i\right). \quad (3.24)$$

3.3 Perturbative expansion

We want to compute the correlation functions by expanding the generating functional (3.8) perturbatively in the coupling constant $g(\eta)$. As g^2 appears in all expressions multiplied by the linear power spectrum $\bar{P}(|\mathbf{k}|)$, the expansion in g^2 is equivalent to the expansion in powers of the initial spectrum used in SPT. Thus, the two approaches should agree when comparing the expressions for the correlators at the same fixed order.

The computation is organized by expanding around the Gaussian part of $\bar{\Gamma}[\Theta]$. We write,

$$\begin{aligned} Z[J; \eta] &= \mathcal{N}^{-1} \int [\mathcal{D}\Theta] \exp \left\{ -\frac{1}{g^2(\eta)} \sum_{n=2}^{\infty} \int \frac{[dk]^n}{n!} \bar{\Gamma}_n \prod_{j=1}^n \Theta(\mathbf{k}_j) \right. \\ &\quad \left. - \sum_{n=1}^{\infty} \int \frac{[dk]^n}{n!} C_n \prod_{j=1}^n \Theta(\mathbf{k}_j) + \int [dk] \Theta(\mathbf{k}) J(-\mathbf{k}) \right\} \\ &= \exp \left\{ -\frac{1}{g^2(\eta)} \sum_{n=3}^{\infty} \int \frac{[dk]^n}{n!} \bar{\Gamma}_n \prod_{j=1}^n \frac{\delta}{\delta J(-\mathbf{k}_j)} - \sum_{n=1}^{\infty} \int \frac{[dk]^n}{n!} C_n \prod_{j=1}^n \frac{\delta}{\delta J(-\mathbf{k}_j)} \right\} Z^{(2)}[J; \eta], \end{aligned} \quad (3.25)$$

where

$$Z^{(2)}[J; \eta] = \mathcal{N}^{-1} \exp \left\{ \frac{g^2(\eta)}{2} \int [dk] \bar{P}(|\mathbf{k}|) J(\mathbf{k}) J(-\mathbf{k}) \right\} \quad (3.26)$$

is the Gaussian part. Taylor expansion of the exponential in (3.25) and use of Wick’s theorem generates Feynman diagrams with the propagator $g^2 \bar{P}(|\mathbf{k}|)$ and vertices $\bar{\Gamma}_n/g^2$, $n \geq 3$ and C_n , $n \geq 1$. The first building blocks for these diagrams are shown in Fig. 1. The Feynman rules are similar to those for a scalar QFT in a 3-dimensional space with Euclidean signature. Unlike an ordinary QFT, the expansion in TSPT contains vertices with an arbitrary number of legs, and all vertices have non-trivial momentum dependence. The latter property implies that in position space the theory is non-local. This non-locality does not lead to any problems in the perturbative expansion and is present also in SPT. In contrast to SPT, time does not flow along the diagrammatic elements, but is taken care of by the time dependence of the coupling constant.

⁸The counterterm C_0 which is also formally generated according to (3.12) gets absorbed into the normalization of the distribution function.

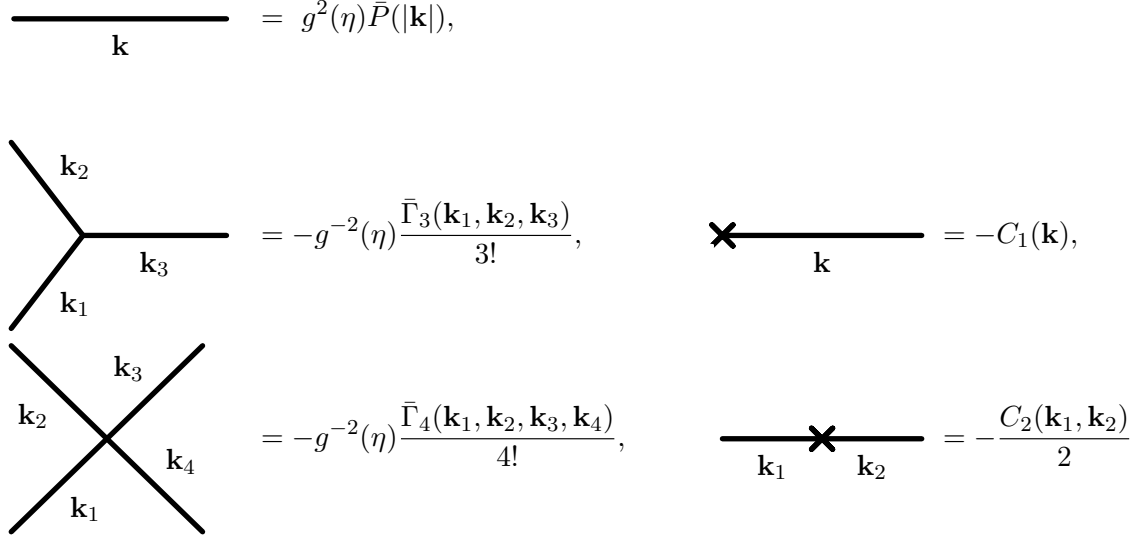


Figure 1. Example of TSPT Feynman diagrams.

It is instructive to consider the tree-level expressions for the 3- and 4-point correlators. Using the diagrams depicted in Fig. 1 one obtains,

$$\langle \Theta_\eta(\mathbf{k}_1) \Theta_\eta(\mathbf{k}_2) \Theta_\eta(\mathbf{k}_3) \rangle^{\text{tree}} = \text{diagram} = -g^4(\eta) \prod_{i=1}^3 \bar{P}(|\mathbf{k}_i|) \bar{\Gamma}_3(\mathbf{k}_1, \mathbf{k}_2, \mathbf{k}_3), \quad (3.27)$$

$$\begin{aligned} \langle \Theta_\eta(\mathbf{k}_1) \Theta_\eta(\mathbf{k}_2) \Theta_\eta(\mathbf{k}_3) \Theta_\eta(\mathbf{k}_4) \rangle^{\text{tree}} &= \text{diagram 1} + \text{diagram 2} \\ &= g^6(\eta) \prod_{i=1}^4 \bar{P}(|\mathbf{k}_i|) \left[-\bar{\Gamma}_4(\mathbf{k}_1, \mathbf{k}_2, \mathbf{k}_3, \mathbf{k}_4) \right. \\ &\quad \left. + \delta^{(3)}\left(\sum_{j=1}^4 \mathbf{k}_j\right) \left(\bar{\Gamma}'_3(\mathbf{k}_1, \mathbf{k}_2, -\mathbf{k}_1 - \mathbf{k}_2) \bar{P}(|\mathbf{k}_1 + \mathbf{k}_2|) \bar{\Gamma}'_3(\mathbf{k}_1 + \mathbf{k}_2, \mathbf{k}_3, \mathbf{k}_4) + \text{perm.} \right) \right], \end{aligned} \quad (3.28)$$

where “perm.” in the last expression stands for the terms obtained by the exchange $\mathbf{k}_2 \leftrightarrow \mathbf{k}_3$ and $\mathbf{k}_2 \leftrightarrow \mathbf{k}_4$. We observe that $\bar{\Gamma}_n$ are identified as one-particle-irreducible (1PI) contributions to the tree-level correlators with amputated external propagators.

As already noted above, the counterterms C_n have the same order in the coupling g as the 1-loop contributions. To understand their role, consider the 1-loop correction to the

average of Θ ,

$$\begin{aligned} \langle \Theta_\eta(\mathbf{k}) \rangle &= \text{---} \bigcirc^{\mathbf{q}} \text{---} + \text{---} \times \text{---} \\ &= -g^2(\eta) \bar{P}(|\mathbf{k}|) \delta^{(3)}(\mathbf{k}) \left[\frac{1}{2} \int [dq] \bar{\Gamma}'_3(\mathbf{k}, \mathbf{q}, -\mathbf{q}) \bar{P}(|\mathbf{q}|) + C'_1(\mathbf{k}) \right]. \end{aligned} \quad (3.29)$$

Using the expressions (B.1a), (B.2a) for $\bar{\Gamma}'_3$ and C'_1 we find that the combination in the square bracket vanishes, provided $I_2(\mathbf{q}, -\mathbf{q}) = 0$. The latter condition is satisfied in the case of fluid dynamics and ZA (cf. eqs. (4.2b), (4.9b), (4.11b)). We conclude that C_1 cancels the unphysical *tadpole* graph. More generally, by inspection of other 1-loop diagrams one finds that C_n cancel certain UV divergent contributions. A detailed study of this cancellation for the Θ -power spectrum at 1-loop can be found in appendix B. Diagrammatically, this can be expressed as

$$P_{\Theta\Theta}^{1\text{-loop}}(\eta; |\mathbf{k}|) = \text{diagram 1} + \text{diagram 2} + \text{diagram 3} \quad (3.30)$$

This calculation allows us to verify explicitly that the total result for $P_{\Theta\Theta}^{1-\text{loop}}$ in TSPT coincides with the standard SPT expression, though the contributions of the individual diagrams in (3.30) are found to be markedly different from those in SPT. In particular, the *daisy* (first term) and *fish* (second term) diagrams in (3.30) contain extra UV divergences, not present in SPT. Some of them are canceled between the *daisy* and the *fish*, whereas the rest are canceled by the counterterm C_2 . We do not consider the appearance of extra UV divergent contributions as a drawback of our formalism, because the fluid description of LSS anyway requires a UV renormalization (see the discussion in the Introduction). Concerning the IR, and in contrast to SPT, all loop diagrams in (3.30) are manifestly IR-finite. In sec. 5 we will prove that this property holds for all building blocks of the TSPT expansion.

To avoid confusion, let us stress that although the C_n -vertices act as counterterms, they differ from generic counterterms of QFT in that their values cannot be adjusted at will: they are fixed unambiguously by the solution of the Liouville equation. They are required to reproduce eventually the SPT result in the perfect fluid case. The UV renormalization of the theory is likely to require additional counterterms to capture the genuine physical effects of the short modes.

3.4 More than one field

So far we have described the TSPT framework for a single field with random initial conditions. In the case of LSS we usually work with two fields — the velocity divergence Θ_η and the density contrast δ_η . The initial conditions for these variables are related: they correspond to the adiabatic linear growing mode. This means that only one of the fields is statistically independent and can act as the argument of the probability distribution function. We choose it to be the velocity divergence Θ_η . The density contrast must be

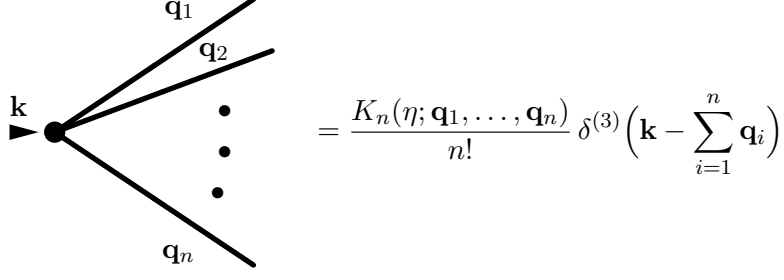


Figure 2. Vertices appearing in the expansion of δ treated as a composite operator.

expressed in terms of Θ_η using the equations of motion.⁹ In the spirit of perturbation theory this relation can be written as Taylor series,

$$\delta_\eta(\mathbf{k}) \equiv \delta[\Theta_\eta; \eta, \mathbf{k}] = \sum_{n=1}^{\infty} \frac{1}{n!} \int [dq]^n K_n(\eta; \mathbf{q}_1, \dots, \mathbf{q}_n) \delta^{(3)}\left(\mathbf{k} - \sum_{i=1}^n \mathbf{q}_i\right) \prod_{j=1}^n \Theta_\eta(\mathbf{q}_j). \quad (3.31)$$

In the next section we will show how to determine the kernels K_n from the equations of fluid mechanics.¹⁰

To compute the correlators involving the density contrast one generalizes the generating functional by inclusion of a source J_δ coupled to δ_η ,

$$Z[J, J_\delta; \eta] = \mathcal{N}^{-1} \int [\mathcal{D}\Theta] \exp \left\{ -\Gamma[\Theta; \eta] + \int [dk] \Theta(\mathbf{k}) J(-\mathbf{k}) + \int [dk] \delta[\Theta; \eta, \mathbf{k}] J_\delta(-\mathbf{k}) \right\}. \quad (3.32)$$

Notice that the sources J and J_δ enter on different footing. While J couples directly to the ‘elementary’ field Θ , J_δ multiplies a series in Θ^n . This means that in the QFT language δ should be interpreted as a *composite* operator. Variation of (3.32) with respect to J_δ produces a set of vertices with multiple legs, which we will denote by a thick dot with an arrow indicating the flow of momentum into or out of the vertex, see Fig. 2.

Let us illustrate this point with the power spectrum for the density field,

$$\langle \delta_\eta(\mathbf{k}) \delta_\eta(\mathbf{k}') \rangle = \frac{\delta^2 Z[J, J_\delta; \eta]}{\delta J_\delta(-\mathbf{k}) \delta J_\delta(-\mathbf{k}')} \Big|_{J, J_\delta=0}. \quad (3.33)$$

We set $K_1 = 1$, which corresponds to the equality between δ_η and Θ_η at the linear level; this is consistent with the adiabatic initial conditions for LSS. Then, the power spectrum of δ at a fixed loop order is given by the same diagrams as the power spectrum of Θ plus a number of extra diagrams containing one or two of the vertices from Fig. 2 with $n \geq 2$. Namely, for one-loop corrections we have,

$$P_{\delta\delta}^{1\text{-loop}}(\eta; |\mathbf{k}|) = P_{\Theta\Theta}^{1\text{-loop}}(\eta; |\mathbf{k}|) + \hat{P}_{\delta\delta}^{1\text{-loop}}(\eta; |\mathbf{k}|), \quad (3.34)$$

⁹In general, for systems with several statistically independent degrees of freedom, the probability density and all the fields must be expressed as functions of the complete set of statistically independent variables.

¹⁰It turns out that in the relevant cases K_n are time-independent, see eqs. (4.8), (4.11). For the sake of generality, we presently keep the argument η in their expressions.

where $P_{\Theta\Theta}^{1-\text{loop}}$ is given by eq. (3.30), whereas the extra contribution has three diagrams

$$\hat{P}_{\delta\delta}^{1-\text{loop}}(\eta; |\mathbf{k}|) = \begin{array}{c} \text{Diagram 1: A circle with momentum } \mathbf{q} \text{ at the top and } \mathbf{q}-\mathbf{k} \text{ at the bottom. An incoming arrow from the left is labeled } K_2 \text{ and } \mathbf{k}. \text{ An outgoing arrow to the right is labeled } \bar{\Gamma}_3 \text{ and } \mathbf{k}. \end{array} + \begin{array}{c} \text{Diagram 2: A circle with momentum } \mathbf{q} \text{ at the top and } \mathbf{q}-\mathbf{k} \text{ at the bottom. Two incoming arrows from the left are both labeled } K_2 \text{ and } \mathbf{k}. \end{array} + \begin{array}{c} \text{Diagram 3: A vertex with an incoming arrow from the left labeled } K_3 \text{ and } \mathbf{k}. \text{ A loop with momentum } \mathbf{q} \text{ is attached to the vertex. An outgoing arrow to the right is labeled } \mathbf{k}. \end{array} \quad (3.35)$$

These diagrams are evaluated in appendix B. As for the Θ case, we show that $P_{\delta\delta}^{1-\text{loop}}$ coincides with the SPT one-loop result.

4 Application to Zel'dovich approximation and exact dynamics

In this section we apply the general formalism developed above to the dark matter fluid. We consider the Zel'dovich approximation and exact dynamics, which are defined by their corresponding evolution kernels I_n and K_n .

4.1 Zel'dovich approximation

In the ZA, the equation (2.2b) is modified by promoting the linear relation between the fields δ and Θ to the non-linear level. Namely, one substitutes $\delta = \Theta$ in the l.h.s. of (2.2b), which allows to decouple the equation for Θ completely from the density field,

$$\dot{\Theta}_\eta(\mathbf{k}) - \Theta_\eta(\mathbf{k}) = \int [dq]^2 \delta^{(3)}(\mathbf{k} - \mathbf{q}_1 - \mathbf{q}_2) \beta(\mathbf{q}_1, \mathbf{q}_2) \Theta_\eta(\mathbf{q}_1) \Theta_\eta(\mathbf{q}_2). \quad (4.1)$$

Comparing this equation to (3.1), (3.2) one identifies,

$$I_1^{ZA} = 1, \quad (4.2a)$$

$$I_2^{ZA}(\mathbf{k}_1, \mathbf{k}_2) = 2\beta(\mathbf{k}_1, \mathbf{k}_2), \quad (4.2b)$$

$$I_n^{ZA} = 0, \quad n \geq 3. \quad (4.2c)$$

In consequence, the recursion relation (3.20b) for the vertices takes a simple form,

$$\bar{\Gamma}_n^{ZA}(\mathbf{k}_1, \dots, \mathbf{k}_n) = -\frac{2}{n-2} \sum_{1 \leq i < j \leq n} \beta(\mathbf{k}_i, \mathbf{k}_j) \bar{\Gamma}_{n-1}^{ZA}(\mathbf{k}_i + \mathbf{k}_j, \mathbf{k}_1, \dots, \check{\mathbf{k}}_i, \dots, \check{\mathbf{k}}_j, \dots, \mathbf{k}_n), \quad (4.3)$$

where the notations $\check{\mathbf{k}}_i, \check{\mathbf{k}}_j$ mean that the kernel $\bar{\Gamma}_{n-1}^{ZA}$ does *not* have these momenta among its arguments. The seed member of the recursion $\bar{\Gamma}_2$ is set by eq. (3.18a).

We now turn to the counterterms C_n . Substituting the expressions (4.2) into eqs. (B.2) from appendix B we obtain,

$$C_1^{ZA}(\mathbf{k}) = 2 \delta^{(3)}(\mathbf{k}) \int [dq] \beta(\mathbf{q}, \mathbf{k}), \quad (4.4a)$$

$$C_2^{ZA}(\mathbf{k}_1, \mathbf{k}_2) = -2 \delta^{(3)}(\mathbf{k}_1 + \mathbf{k}_2) \beta(\mathbf{k}_1, \mathbf{k}_2) \int [dq] \beta(\mathbf{q}, \mathbf{k}_1 + \mathbf{k}_2). \quad (4.4b)$$

Note that the asymptotic behavior $\beta(\mathbf{k}, \mathbf{q}) = O(q/k)$ at $q \rightarrow \infty$ implies that the integrals on the r.h.s. are UV divergent. In principle, they should be regularized by introduction of

a UV cutoff. We won't need the details of this regularization: in the actual computations the divergences cancel when summed with the loop contributions, see appendix B. In ZA, the situation is actually even simpler. Using the property

$$\lim_{p \rightarrow 0} \beta(\mathbf{q}, \mathbf{p}) \beta(\mathbf{k}, -\mathbf{k} + \mathbf{p}) = \lim_{p \rightarrow 0} \frac{(\mathbf{q} \cdot \mathbf{p})}{p^2} \frac{p^2}{k^2} = 0, \quad (4.5)$$

we infer that C_2^{ZA} vanishes. Then, the recursion relation (3.23) together with eq. (4.2c) imply that all C_n with $n > 2$ vanish as well. We conclude that in ZA only the first counterterm C_1 is non-zero. As discussed in sec. 3.3, its role is precisely to cancel the *tadpole* contributions. Thus, in ZA one can forget both about the counterterms and tadpoles in the diagrammatic expansion.

4.1.1 The density field

The vertices $\bar{\Gamma}_n$ are sufficient to compute the correlators of the velocity dispersion Θ in ZA. For the correlators of the density field δ we need to know also the kernels K_n . Substituting the representation (3.31) into the continuity equation (2.2a) we find that these satisfy a system of linear differential equations,

$$\dot{K}_1^{ZA}(\eta; \mathbf{k}) + K_1^{ZA}(\eta; \mathbf{k}) = 1, \quad (4.6a)$$

$$\begin{aligned} \dot{K}_2^{ZA}(\eta; \mathbf{k}_1, \mathbf{k}_2) + 2K_2^{ZA}(\eta; \mathbf{k}_1, \mathbf{k}_2) &= \alpha(\mathbf{k}_1, \mathbf{k}_2) K_1^{ZA}(\eta; \mathbf{k}_2) + \alpha(\mathbf{k}_2, \mathbf{k}_1) K_1^{ZA}(\eta; \mathbf{k}_1) \\ &\quad - 2\beta(\mathbf{k}_1, \mathbf{k}_2) K_1^{ZA}(\eta; \mathbf{k}_1 + \mathbf{k}_2), \end{aligned} \quad (4.6b)$$

$$\begin{aligned} \dot{K}_n^{ZA}(\eta; \mathbf{k}_1, \dots, \mathbf{k}_n) + nK_n^{ZA}(\eta; \mathbf{k}_1, \dots, \mathbf{k}_n) \\ + 2 \sum_{1 \leq i < j \leq n} \beta(\mathbf{k}_i, \mathbf{k}_j) K_{n-1}^{ZA}(\eta; \mathbf{k}_i + \mathbf{k}_j, \mathbf{k}_1, \dots, \check{\mathbf{k}}_i, \dots, \check{\mathbf{k}}_j, \dots, \mathbf{k}_n) \\ = \sum_{i=1}^n \alpha\left(\mathbf{k}_i, \sum_{1 \leq j \leq n, j \neq i} \mathbf{k}_j\right) K_{n-1}^{ZA}(\eta; \mathbf{k}_1, \dots, \check{\mathbf{k}}_i, \dots, \mathbf{k}_n), \quad n \geq 3. \end{aligned} \quad (4.6c)$$

For the adiabatic mode $\delta_\eta = \Theta_\eta$ at $\eta \rightarrow -\infty$. This corresponds to the initial conditions on the kernels,

$$\lim_{\eta \rightarrow -\infty} K_1(\eta) = 1, \quad \lim_{\eta \rightarrow -\infty} K_n(\eta) e^{(n-1)\eta} = 0, \quad n \geq 2. \quad (4.7)$$

The solution of (4.6) that satisfy these initial conditions is time-independent and is given by the recursions formulas,

$$K_1^{ZA} = 1, \quad (4.8a)$$

$$K_2^{ZA}(\mathbf{k}_1, \mathbf{k}_2) = 1 - \frac{(\mathbf{k}_1 \cdot \mathbf{k}_2)^2}{k_1^2 k_2^2} \equiv \sin^2(\mathbf{k}_1, \mathbf{k}_2), \quad (4.8b)$$

$$\begin{aligned} K_n^{ZA}(\mathbf{k}_1, \dots, \mathbf{k}_n) &= \frac{1}{n} \left[\sum_{i=1}^n \alpha\left(\mathbf{k}_i, \sum_{1 \leq j \leq n, j \neq i} \mathbf{k}_j\right) K_{n-1}^{ZA}(\mathbf{k}_1, \dots, \check{\mathbf{k}}_i, \dots, \mathbf{k}_n) \right. \\ &\quad \left. - 2 \sum_{1 \leq i < j \leq n} \beta(\mathbf{k}_i, \mathbf{k}_j) K_{n-1}^{ZA}(\mathbf{k}_i + \mathbf{k}_j, \mathbf{k}_1, \dots, \check{\mathbf{k}}_i, \dots, \check{\mathbf{k}}_j, \dots, \mathbf{k}_n) \right], \quad n \geq 3. \end{aligned} \quad (4.8c)$$

To sum up, eqs. (4.3), (4.8) determine all ingredients of the TSPT diagrammatic expansion within Zel'dovich approximation.

4.2 Exact dynamics

We now repeat the above derivation for exact dynamics. In this case the equations for the kernels I_n cannot be decoupled and must be solved together with the equations for K_n . We proceed as follows. First, we use eq. (2.2b) to express I_n in terms of K_n . Substituting the expansion (3.31) we obtain,¹¹

$$I_1(\eta; \mathbf{k}) = -\frac{1}{2} + \frac{3}{2}K_1(\eta; \mathbf{k}) , \quad (4.9a)$$

$$I_2(\eta; \mathbf{k}_1, \mathbf{k}_2) = 2\beta(\mathbf{k}_1, \mathbf{k}_2) + \frac{3}{2}K_2(\eta; \mathbf{k}_1, \mathbf{k}_2) , \quad (4.9b)$$

$$I_n(\eta; \mathbf{k}_1, \dots, \mathbf{k}_n) = \frac{3}{2}K_n(\eta; \mathbf{k}_1, \dots, \mathbf{k}_n) , \quad n \geq 3 . \quad (4.9c)$$

Next, we insert the expansions (3.2), (3.31) into (2.2a). After a straightforward calculation one arrives to a chain of differential equations,

$$\dot{K}_1(\eta; \mathbf{k}) + I_1(\eta; \mathbf{k})K_1(\eta; \mathbf{k}) = 1 , \quad (4.10a)$$

$$\begin{aligned} \dot{K}_n(\eta; \mathbf{k}_1, \dots, \mathbf{k}_n) + \sum_{m=1}^n \frac{1}{m!(n-m)!} \sum_{\sigma} I_m(\eta; \mathbf{k}_{\sigma(1)}, \dots, \mathbf{k}_{\sigma(m)}) \\ \times K_{n-m+1} \left(\sum_{l=1}^m \mathbf{k}_{\sigma(l)}, \mathbf{k}_{\sigma(m+1)}, \dots, \mathbf{k}_{\sigma(n)} \right) \\ = \sum_{i=1}^n \alpha \left(\mathbf{k}_i, \sum_{1 \leq j \leq n, j \neq i} \mathbf{k}_j \right) K_{n-1}(\mathbf{k}_1, \dots, \check{\mathbf{k}}_i, \dots, \mathbf{k}_n) , \quad n \geq 2 . \end{aligned} \quad (4.10b)$$

Using eqs. (4.9) we obtain a closed system for the kernels K_n . Note that the equation for the n -th kernel depends only on K_m with $m \leq n$, so the system can be solved exactly. The adiabatic initial conditions (4.7) uniquely fix the solution, which as in ZA case, is found to be time-independent. We obtain the recursion relations,

$$K_1 = 1 , \quad (4.11a)$$

$$K_2(\mathbf{k}_1, \mathbf{k}_2) = \frac{4}{7} \sin^2(\mathbf{k}_1, \mathbf{k}_2) , \quad (4.11b)$$

$$\begin{aligned} K_n(\mathbf{k}_1, \dots, \mathbf{k}_n) = \frac{2}{2n+3} \left[\sum_{i=1}^n \alpha \left(\mathbf{k}_i, \sum_{1 \leq j \leq n, j \neq i} \mathbf{k}_j \right) K_{n-1}(\mathbf{k}_1, \dots, \check{\mathbf{k}}_i, \dots, \mathbf{k}_n) \right. \\ - \sum_{1 \leq i < j \leq n} \left(2\beta(\mathbf{k}_i, \mathbf{k}_j) + \frac{3}{2}K_2(\mathbf{k}_i, \mathbf{k}_j) \right) K_{n-1}(\mathbf{k}_i + \mathbf{k}_j, \mathbf{k}_1, \dots, \check{\mathbf{k}}_i, \dots, \check{\mathbf{k}}_j, \dots, \mathbf{k}_n) \\ \left. - \frac{3}{2} \sum_{m=3}^{n-1} \frac{1}{m!(n-m)!} \sum_{\sigma} K_m(\mathbf{k}_{\sigma(1)}, \dots, \mathbf{k}_{\sigma(m)}) K_{n-m+1} \left(\sum_{l=1}^m \mathbf{k}_{\sigma(l)}, \mathbf{k}_{\sigma(m+1)}, \dots, \mathbf{k}_{\sigma(n)} \right) \right] , \\ n \geq 3 . \end{aligned} \quad (4.11c)$$

¹¹Recall that we work in the approximation $\Omega_m/f^2 = 1$.

The kernels I_n are then retrieved from (4.9). Note that (4.11a) implies $I_1 = 1$, justifying the assumption in eq. (3.14). Although the recursion relation (4.11c) becomes complicated at higher n , this does not pose an obstruction for practical computations, which involve only a few kernels. For example, to evaluate 1-loop (2-loop) corrections to the power-spectrum one needs the kernels up to K_3 (K_5). It is worth mentioning also that if one knows already the SPT kernels, the K_n kernels can be directly found from them, see appendix A.

Once the kernels K_n , I_n are known, it is straightforward to construct the vertices $\bar{\Gamma}_n$ and the counterterms C_n using the general expressions (3.20b), (3.23). For future reference, let us single out the term containing I_2 on the r.h.s. of eq. (3.20b),

$$\begin{aligned} \bar{\Gamma}_n(\mathbf{k}_1, \dots, \mathbf{k}_n) = & \frac{-1}{n-2} \sum_{1 \leq i < j \leq n} \left(2\beta(\mathbf{k}_i, \mathbf{k}_j) + \frac{3}{2} K_2(\mathbf{k}_i, \mathbf{k}_j) \right) \bar{\Gamma}_{n-1}(\mathbf{k}_i + \mathbf{k}_j, \mathbf{k}_1, \dots, \check{\mathbf{k}}_i, \dots, \check{\mathbf{k}}_j, \dots, \mathbf{k}_n) \\ & - \frac{3}{2(n-2)} \sum_{m=3}^{n-1} \frac{1}{m!(n-m)!} \sum_{\sigma} K_m(\mathbf{k}_{\sigma(1)}, \dots, \mathbf{k}_{\sigma(m)}) \bar{\Gamma}_{n-m+1} \left(\sum_{l=1}^m \mathbf{k}_{\sigma(l)}, \mathbf{k}_{\sigma(m+1)}, \dots, \mathbf{k}_{\sigma(n)} \right). \end{aligned} \quad (4.12)$$

Finally, for the first two counterterms we have,

$$C_1(\mathbf{k}) = \delta^{(3)}(\mathbf{k}) \int [dq] \left(2\beta(\mathbf{q}, \mathbf{k}) + \frac{3}{2} K_2(\mathbf{q}, \mathbf{k}) \right), \quad (4.13a)$$

$$C_2(\mathbf{k}_1, \mathbf{k}_2) = \frac{3}{4} \delta^{(3)}(\mathbf{k}_1 + \mathbf{k}_2) \int [dq] K_3(\mathbf{q}, \mathbf{k}_1, \mathbf{k}_2), \quad (4.13b)$$

where we used the general formulas (B.2) and the property (B.3) that can be easily verified using (4.9b), (4.11b). We observe that, unlike ZA, the counterterm C_2 does not vanish. The same is also true for higher counterterms. They must be properly taken into account in the loop computations.

5 Soft limits and infrared safety

Even if the equal time correlators are the same in TSPT and SPT, the intermediate quantities required to compute them are very different. As pointed out in the Introduction, in SPT individual diagrams contain unphysical singularities at low-momenta that cancel only when all the diagrams are added up. This complicates the calculations at high loop and hampers the development of diagrammatic resummation techniques which would be desirable to correctly capture the physical effects of IR modes. We show in this section that this problem is absent in TSPT where the individual elements are already IR-safe.

5.1 Vertices with soft momenta

We want to show that the vertices $\bar{\Gamma}_n$, C_n and K_n appearing in the TSPT diagrammatic expansion are bounded at finite values of their arguments¹². Then, the loop integrals will

¹² More precisely, we will show that these functions do not have any poles associated to the dynamical coupling between the hard and soft modes. The vertices $\bar{\Gamma}_n$ (and only them) being inversely proportional to the linear power spectrum, may, in principle, diverge if the latter vanishes at some values of the momentum.

be free from any IR divergences as long as the power spectrum, which plays the role of the propagator, behaves as¹³ $\bar{P}(|\mathbf{q}|) \propto q^\nu$ with $\nu > -3$ at $\mathbf{q} \rightarrow 0$. We consider ZA and ED in parallel. Recall that the *leading* IR behavior in these two cases is identical [13, 37].

Let us first discuss the K_n vertices. One observes that K_2 given by (4.8b) or (4.11b) is manifestly bounded. The proof proceeds by induction. Assume that all K_m with $m < n$ are bounded. From the recursion relations (4.8c), (4.11c) it is clear that the only potential sources of singularities in K_n are the poles of the kernels α and β occurring when either the first argument of α or one of the two arguments of β goes to zero, see eqs. (2.4). Thus, K_n could potentially have a singularity only if some of the momenta among its arguments vanish. To analyze this limit, let us split all arguments of K_n into ‘hard’ momenta $\mathbf{k}_1, \dots, \mathbf{k}_l$ that we keep fixed, and ‘soft’ $\mathbf{q}_1, \dots, \mathbf{q}_{n-l}$ which are uniformly sent to zero,

$$\mathbf{q}_s = \epsilon \mathbf{q}'_s, \quad \epsilon \rightarrow 0, \quad \mathbf{q}'_s - \text{fixed}. \quad (5.1)$$

Focusing on the dangerous terms we obtain,¹⁴

$$\begin{aligned} K_n(\mathbf{k}_1, \dots, \mathbf{k}_l, \mathbf{q}_1, \dots, \mathbf{q}_{n-l}) &= A_n \left[\sum_{s=1}^{n-l} \alpha\left(\mathbf{q}_s, \sum_{i=1}^l \mathbf{k}_i\right) K_{n-1}(\mathbf{k}_1, \dots, \mathbf{k}_l, \mathbf{q}_1, \dots, \check{\mathbf{q}}_s, \dots, \mathbf{q}_{n-l}) \right. \\ &\quad \left. - 2 \sum_{s=1}^{n-l} \sum_{i=1}^l \beta(\mathbf{q}_s, \mathbf{k}_i) K_{n-1}(\mathbf{k}_1, \dots, \mathbf{k}_i + \mathbf{q}_s, \dots, \mathbf{k}_l, \mathbf{q}_1, \dots, \check{\mathbf{q}}_s, \dots, \mathbf{q}_{n-l}) \right] + O(\epsilon^0) \\ &= A_n \sum_{s=1}^{n-l} \left[\alpha\left(\mathbf{q}_s, \sum_{i=1}^l \mathbf{k}_i\right) - 2 \sum_{i=1}^l \beta(\mathbf{q}_s, \mathbf{k}_i) \right] K_{n-1}(\mathbf{k}_1, \dots, \mathbf{k}_l, \mathbf{q}_1, \dots, \check{\mathbf{q}}_s, \dots, \mathbf{q}_{n-l}) + O(\epsilon^0), \end{aligned} \quad (5.2)$$

where

$$A_n = \begin{cases} \frac{1}{n} & \text{for ZA,} \\ \frac{2}{2n+3} & \text{for ED,} \end{cases}$$

and $O(\epsilon^0)$ stands for terms that are finite in the limit $\epsilon \rightarrow 0$. The key observation is that the poles of α and β at $\mathbf{q}_s \rightarrow 0$ cancel in the combination inside the brackets in the last line of (5.2). Thus, this combination is $O(\epsilon^0)$ and the vertex K_n is IR-finite.

We turn to $\bar{\Gamma}_n$. The proof again goes by induction. $\bar{\Gamma}_2$ is given by eq. (3.18a) and is bounded if the power spectrum does not vanish. In the realistic cosmology this condition is formally violated at $q \rightarrow 0$ where $\bar{P}(|\mathbf{q}|)$ behaves linearly. However, as explained in the footnote 12, this does not pose a threat to the IR-safety. For the sake of the argument, we are going to assume that the power spectrum is bounded from below, being concerned only with those divergences that might arise from the dynamical coupling between the hard and

In the real world this happens at low momenta where $\bar{P}(|\mathbf{q}|) \propto q$. However, these divergences cancel in the *individual* TSPT diagrams where the vertices are multiplied by positive powers of the propagator proportional to $\bar{P}(|\mathbf{q}|)$. Furthermore, we show in Appendix C that $\bar{\Gamma}_n$ are finite if at least two of their arguments are hard and the power spectrum behaves at small q as $P(|\mathbf{q}|) \propto q^\nu$ with $\nu \leq 2$.

¹³Recall that individual loop integrals in SPT do not have IR divergences if $\nu > -1$ [12].

¹⁴Note that we do not write the terms where both arguments of α or β are soft, as they are bounded in the limit $\epsilon \rightarrow 0$, see eqs. (2.4).

soft modes. The generalization of the proof to the case when the power spectrum behaves as $\bar{P}(|\mathbf{q}|) \propto q^\nu$ with $\nu \leq 2$ at $q \rightarrow 0$ is given in Appendix C.

Assume that all $\bar{\Gamma}_m$ with $m < n$ have been already shown to be finite. Then, the only contributions in the recursion relations (4.3), (4.12) that could induce singularities of $\bar{\Gamma}_n$ are the terms containing the kernels β . Note that they are identical in ZA and ED. Splitting again the arguments of $\bar{\Gamma}_n$ into hard and soft, with soft momenta \mathbf{q}_s going uniformly to zero as in (5.1), we isolate the dangerous part,

$$\bar{\Gamma}_n(\mathbf{k}_1, \dots, \mathbf{k}_l, \mathbf{q}_1, \dots, \mathbf{q}_{n-l}) = \frac{-2}{n-2} \sum_{s=1}^{n-l} \left[\sum_{i=1}^l \beta(\mathbf{q}_s, \mathbf{k}_i) \right] \bar{\Gamma}_{n-1}(\mathbf{k}_1, \dots, \mathbf{k}_l, \mathbf{q}_1, \dots, \check{\mathbf{q}}_i, \dots, \mathbf{q}_{n-l}) + O(\epsilon^0) \quad (5.3)$$

For the sum in brackets we have,

$$\sum_{i=1}^l \beta(\mathbf{q}_s, \mathbf{k}_i) = \frac{(\mathbf{q}_s \cdot \sum_{i=1}^l \mathbf{k}_i)}{2q_s^2} + O(\epsilon^0) .$$

Recall now that, due to the momentum conservation, the sum of all momenta entering into the vertex $\bar{\Gamma}_n$ must be zero, see eqs. (3.24). This implies,

$$\sum_{i=1}^l \mathbf{k}_i = - \sum_{s=1}^{n-l} \mathbf{q}_s = O(\epsilon) \quad \implies \quad \sum_{i=1}^l \beta(\mathbf{q}_s, \mathbf{k}_i) = O(\epsilon^0) . \quad (5.4)$$

One concludes that all poles on the r.h.s. of (5.3) cancel, and $\bar{\Gamma}_n$ is also IR-safe.

Finally, this argument can be repeated essentially without changes to demonstrate the finiteness of C_n using the recursion relation (3.23).

5.2 Relation to the equivalence principle

The IR-safety of equal-time correlators is known to be closely related to the symmetry of LSS dynamics [13] that can be traced back to the equivalence principle [14]. This symmetry has been used to derive the consistency conditions for the IR structure of correlation functions that do not rely on any specifics of the fluid approximation [14, 18, 19, 38]. Here we explore the implications of this symmetry for TSPT. This approach is similar to that of [39] where it was applied to derive relations between inflationary correlators. Treating the logarithm of the probability distribution $\Gamma[\Theta; \eta]$ as an ‘effective action’ of a 3-dimensional Euclidean QFT, we require it to be invariant under the symmetry transformations and derive the corresponding conditions on the vertices Γ_n^{tot} (Ward identities). We do not rely on any particular form of the equations of motion in this section, so our results will be valid for any system satisfying the relevant symmetry.

Consider the coordinate transformation,

$$\eta \mapsto \eta, \quad \mathbf{x} \mapsto \tilde{\mathbf{x}} = \mathbf{x} - \epsilon^\eta \nabla \Phi_L(\mathbf{x}), \quad (5.5a)$$

where the function $\Phi_L(\mathbf{x})$ describes a long-wavelength perturbation. Accordingly, its Fourier transform $\Phi_L(\mathbf{k})$ has support only at low momenta $k < 1/L$. The density contrast

transforms as a scalar under (5.5a), while the velocity divergence acquires an inhomogeneous piece due to the time dependence of the coordinate shift,

$$\tilde{\delta}_\eta(\tilde{\mathbf{x}}) = \delta_\eta(\mathbf{x}) , \quad \tilde{\Theta}_\eta(\tilde{\mathbf{x}}) = \Theta_\eta(\mathbf{x}) + e^\eta \nabla^2 \Phi_L(\mathbf{x}) . \quad (5.5b)$$

We will be eventually interested in the limit $L \rightarrow \infty$, assuming a constant limiting value for the gradient of Φ_L ,

$$\nabla \Phi_L(\mathbf{x}) \rightarrow \mathbf{a} \quad \Longleftrightarrow \quad \mathbf{k} \Phi_L(\mathbf{k}) \rightarrow -i\mathbf{a} \delta^{(3)}(\mathbf{k}) , \quad \text{at } L \rightarrow \infty . \quad (5.6)$$

In this limit one can write the transformations (5.5b) in Fourier space as,

$$\tilde{\delta}_\eta(\mathbf{k}) = \delta_\eta(\mathbf{k}) e^{i(\mathbf{a} \cdot \mathbf{k}) e^\eta} (1 + O(1/L)) , \quad (5.7a)$$

$$\tilde{\Theta}_\eta(\mathbf{k}) = (\Theta_\eta(\mathbf{k}) - e^\eta k^2 \Phi_L(\mathbf{k})) e^{i(\mathbf{a} \cdot \mathbf{k}) e^\eta} (1 + O(1/L)) . \quad (5.7b)$$

Assume that the original fields $\delta_\eta(\mathbf{k})$, $\Theta_\eta(\mathbf{k})$ are solutions of the hydrodynamic equations (2.2). Then it is straightforward to check that the transformed fields (5.7) also satisfy these equations up to terms that vanish as $O(1/L)$. Thus, in the limit (5.6) the transformations (5.7) become a symmetry of the equations of motion¹⁵. Importantly, this invariance crucially relies on the presence of the inhomogeneous piece in the Θ -transformation (5.7b). Although this term vanishes in the limit (5.6), it gets multiplied in the equations of motion by the kernels α and β that have poles at low momenta. These poles cancel one factor of k in $k^2 \Phi_L(\mathbf{k})$, which leads to a finite contributions at $L \rightarrow \infty$. It should be also stressed that we have not assumed the gradient of the long mode to be small, so the invariance holds to arbitrary order in \mathbf{a} .

As discussed in [14, 38], the transformation (5.5) corresponds to superimposing a long-wavelength adiabatic growing mode on top of the original perturbation. The function $\Phi_L(\mathbf{x})$ is proportional to the initial value of the long-mode gravitational potential. The invariance of the dynamics in the limit (5.6) then follows from the equivalence principle: the transformation (5.5) describes the free fall of the short-scale perturbation in the gravitational field of the long mode, which does not affect the local physics. Therefore, this invariance is valid beyond the fluid approximation and holds for any theory obeying the equivalence principle.

The above interpretation implies that the probability to find the transformed field $\tilde{\Theta}_\eta(\mathbf{k})$ in the statistical ensemble is equal to the probability of finding the original field $\Theta_\eta(\mathbf{k})$ times the probability to find the long mode¹⁶. This leads to the relation,

$$\Gamma[\tilde{\Theta}_\eta; \eta] = \Gamma[\Theta_\eta, \eta] + \Gamma[\Theta_{\eta,L}; \eta] , \quad (5.8)$$

¹⁵Actually, the symmetry group of eqs. (2.2) is much broader [18, 38]. They are invariant in the limit (5.6) under the transformations,

$$\tilde{\delta}_\eta(\mathbf{k}) = \delta_\eta(\mathbf{k}) e^{i(\mathbf{a} \cdot \mathbf{k}) \xi(\eta)} , \quad \tilde{\Theta}_\eta(\mathbf{k}) = (\Theta_\eta(\mathbf{k}) - \dot{\xi}(\eta) k^2 \Phi_L(\mathbf{k})) e^{i(\mathbf{a} \cdot \mathbf{k}) \xi(\eta)} ,$$

with an arbitrary function $\xi(\eta)$. However, only the time dependence used in (5.7) can be embedded into the full generally relativistic description [14, 38].

¹⁶Here we use that the initial distribution is Gaussian, so that the long and short modes are statistically independent.

where $\Theta_{\eta,L}(\mathbf{k}) = -e^{\eta k^2} \Phi_L(\mathbf{k}) e^{i(\mathbf{a} \cdot \mathbf{k}) e^\eta}$. The long mode is in the linear regime, implying that its statistical weight is essentially Gaussian (see eqs. (3.18a), (3.20a)),

$$\Gamma[\Theta_{\eta,L}; \eta] = \frac{e^{-2\eta}}{2} \int [dk] \frac{\Theta_{\eta,L}(\mathbf{k}) \Theta_{\eta,L}(-\mathbf{k})}{\bar{P}(|\mathbf{k}|)} = \frac{1}{2} \int [dk] \frac{k^4 \Phi_L(\mathbf{k}) \Phi_L(-\mathbf{k})}{\bar{P}(|\mathbf{k}|)},$$

As expected, it does not depend on time. Moreover, unless $\bar{P}(|\mathbf{k}|)$ vanishes at $k \rightarrow 0$ as k^2 or faster, we have,

$$\lim_{L \rightarrow \infty} \Gamma[\Theta_{\eta,L}; \eta] = 0.$$

Comparing with (5.8) we obtain that the weight Γ must be invariant in the limit (5.6),

$$\lim_{L \rightarrow \infty} \Gamma[\tilde{\Theta}_\eta; \eta] = \Gamma[\Theta_\eta; \eta]. \quad (5.9)$$

This condition is a consequence of equivalence principle and initial Gaussian statistics.

Using the power-series representation for Γ yields a set of equations in the limit (5.6),

$$\lim_{L \rightarrow \infty} \int [dq]^{n-l} \Gamma_n^{tot}(\eta; \mathbf{k}_1, \dots, \mathbf{k}_l, \mathbf{q}_1, \dots, \mathbf{q}_{n-l}) \prod_{s=1}^{n-l} (q_s^2 \Phi_L(\mathbf{q}_s)) = 0 \quad (5.10)$$

for all $1 \leq l \leq n-1$. This translates into the following conditions on the vertices,

$$\lim_{\epsilon \rightarrow 0} \epsilon^{n-l} \Gamma_n^{tot}(\eta; \mathbf{k}_1, \dots, \mathbf{k}_l, \epsilon \mathbf{q}_1, \dots, \epsilon \mathbf{q}_{n-l}) = 0, \quad 1 \leq l \leq n-1. \quad (5.11)$$

These conditions imply that the vertices Γ_n^{tot} cannot have poles of order $(n-l)$ or higher when $(n-l)$ of their momenta become soft. However, they do not forbid, in principle, poles of lower orders. In this respect, they are weaker than the perturbative result of sec. 5.1 which states that Γ_n^{tot} do not have any singularities whatsoever. They are, however, more powerful in the sense that they are valid beyond the ideal fluid approximation.

As the last remark, we note that the equivalence principle also constrains the IR properties of the vertices K_n . Substituting the transformation (5.7) into the relation (3.31) between δ and Θ and requiring it to be invariant in the limit $L \rightarrow \infty$, we obtain the same condition as eq. (5.11) with Γ_n^{tot} replaced by K_n .

6 Discussion

We have proposed a new perturbative approach to non-linear structure formation that overcomes some of the drawbacks of standard Eulerian perturbation theory. Rather than studying the time evolution of cosmological fields, we consider the time evolution of their probability distribution, as is common in statistical mechanics. Starting from generic hydrodynamical equations of motions for the density and velocity fields we derive the analogue of the Liouville continuity equation that governs the time evolution of the probability distribution function. We have shown that this equation can formally be solved exactly, without any need for assuming an ad-hoc truncation. Equal-time observables such as the power spectrum can be computed perturbatively based on the time-evolved probability distribution. At this stage time plays the role of an external parameter, which suggests

the name Time-Sliced Perturbation Theory (TSPT). We have developed the diagrammatic technique within this approach and worked out its ingredients for the Zel’dovich approximation and the exact Eulerian dynamics with an initially Gaussian distribution. The formulation proposed here admits a representation in terms of a generating functional for equal-time correlation functions, that is formally similar to QFT in three-dimensional Euclidean space, and therefore allows to apply QFT techniques in a transparent way.

An important property of this formulation is that all building blocks entering the perturbative computation are by themselves infrared safe. This is a direct consequence of the fact that time-evolution and statistical averaging are disentangled. The perturbative expansion then involves only equal-time quantities that are protected by the underlying symmetries related to the equivalence principle. Compared to the standard Eulerian formulation of perturbation theory (SPT), this facilitates the application of diagrammatic resummation techniques.

In this work we focussed on the general formalism, demonstrated the infrared safety, and worked out a sample calculation for an ideal pressureless fluid. However, we paid special attention to keep the derivation generic. It can indeed be easily adapted to describe non-ideal fluids and is particularly suited to include primordial non-Gaussianity. Furthermore, if the hydrodynamical evolution equations were supplemented by a stochastic force (noise term), this could be accounted for by replacing the Liouville equation for the distribution function by a Fokker-Planck equation.

The properties discussed above suggest that TSPT is suitable to address shortcomings of perturbation theory, in particular, infrared resummation, which is important to capture the shape of the baryon acoustic peak [32]. This resummation can be systematically formulated at the level of Feynman diagrams within TSPT, by virtue of its advantageous infrared properties. Furthermore, due to the similarities with Euclidean QFT, it is a natural framework to apply methods of renormalization group evolution in order to better understand the UV sensitivity of the perturbative expansion.

For realistic applications the method should be extended to include redshift space distortions and the effects of baryons. We leave this for future research. Let us note that the formulation based on a time-evolved probability distribution function appears convenient for the description of biased tracers.

Acknowledgements

We thank D. Gorbunov, E. Pajer, R. Porto, P. De Los Rios, F. Vernizzi and Y. Zenkevich for useful discussions. D.B. acknowledges the hospitality of CCPP at NYU while this work was in preparation. S.S. thanks Kavli Institute for Theoretical Physics at Santa Barbara for hospitality during the initial stage of this project (the visit to KITP was supported in part by the National Science Foundation under Grant NSF PHY11-25915). This work was supported by the Swiss National Science Foundation (M.I. and S.S.) and the RFBR grants 14-02-31435 and 14-02-00894 (M.I.).

A TSPT kernels from SPT

Here we show how the quantities appearing in TSPT can be related to the SPT kernels F_n , G_n . In SPT one expresses the fields at a given moment of time in terms of their initial values,

$$\delta_\eta(\mathbf{k}) = \sum_{n=1} e^{n\eta} \int [dq]^n F_n(\mathbf{q}_1, \dots, \mathbf{q}_n) \delta^{(3)}\left(\mathbf{k} - \sum_{i=1}^n \mathbf{q}_i\right) \prod_{j=1}^n \Theta_0(\mathbf{q}_j), \quad (\text{A.1a})$$

$$\Theta_\eta(\mathbf{k}) = \sum_{n=1} e^{n\eta} \int [dq]^n G_n(\mathbf{q}_1, \dots, \mathbf{q}_n) \delta^{(3)}\left(\mathbf{k} - \sum_{i=1}^n \mathbf{q}_i\right) \prod_{j=1}^n \Theta_0(\mathbf{q}_j). \quad (\text{A.1b})$$

To connect the K_n kernels with the F_n and G_n kernels consider eq. (3.31). This produces a hierarchy of equations for the K_n kernels, that can be solved iteratively. For instance, the first non trivial relations are,

$$K_2(\mathbf{q}_1, \mathbf{q}_2) = 2(F_2(\mathbf{q}_1, \mathbf{q}_2) - G_2(\mathbf{q}_1, \mathbf{q}_2)), \quad (\text{A.2a})$$

$$K_3(\mathbf{q}_1, \mathbf{q}_2, \mathbf{q}_3) = 6(F_3(\mathbf{q}_1, \mathbf{q}_2, \mathbf{q}_3) - G_3(\mathbf{q}_1, \mathbf{q}_2, \mathbf{q}_3)) - 2 \sum_{1 \leq i < j \leq 3} G_2(\mathbf{q}_i, \mathbf{q}_j) K_2(\mathbf{q}_i + \mathbf{q}_j, \mathbf{q}_l) \Big|_{l \neq i, j} \quad (\text{A.2b})$$

The formulas for I_n are derived by substituting the expression (A.1b) into the equations (3.1) and (3.2). For the lowest kernels one has,

$$I_2(\mathbf{q}_1, \mathbf{q}_2) = 2G_2(\mathbf{q}_1, \mathbf{q}_2), \quad (\text{A.3a})$$

$$I_3(\mathbf{q}_1, \mathbf{q}_2, \mathbf{q}_3) = 12G_3(\mathbf{q}_1, \mathbf{q}_2, \mathbf{q}_3) - 4 \sum_{1 \leq i < j \leq 3} G_2(\mathbf{q}_i, \mathbf{q}_j) G_2(\mathbf{q}_i + \mathbf{q}_j, \mathbf{q}_l) \Big|_{l \neq i, j}. \quad (\text{A.3b})$$

Since the vertices $\bar{\Gamma}_n$ and counterterms C_n are expressed in TSPT through I_n and K_n the above relations allow to write them as combinations of the SPT kernels.

B 1-loop results and comparison with SPT

In this appendix we perform an explicit computation of 1-loop corrections to the Θ and δ power spectra in TSPT. First we summarize the expressions for the vertices that we will need in the calculation. Using the general formula (3.20b) we obtain the 3- and 4-point vertices,

$$\bar{\Gamma}_3(\mathbf{k}_1, \mathbf{k}_2, \mathbf{k}_3) = -\delta^{(3)}\left(\sum \mathbf{k}_i\right) \left[\frac{I_2(\mathbf{k}_1, \mathbf{k}_2)}{\bar{P}(|\mathbf{k}_3|)} + \text{cycl.} \right], \quad (\text{B.1a})$$

$$\begin{aligned} \bar{\Gamma}_4(\mathbf{k}_1, \mathbf{k}_2, \mathbf{k}_3, \mathbf{k}_4) = \delta^{(3)}\left(\sum \mathbf{k}_i\right) & \left\{ \frac{1}{2} \sum_{1 \leq i < j \leq 4} I_2(\mathbf{k}_i, \mathbf{k}_j) \left[\frac{I_2(\mathbf{k}_i + \mathbf{k}_j, \mathbf{k}_l)}{\bar{P}(|\mathbf{k}_m|)} + \text{cycl.} \right] \right\}_{\substack{l < m \\ l, m \neq i, j}} \\ & - \frac{1}{2} \left[\frac{I_3(\mathbf{k}_1, \mathbf{k}_2, \mathbf{k}_3)}{\bar{P}(|\mathbf{k}_4|)} + \text{cycl.} \right] \Big\}, \quad (\text{B.1b}) \end{aligned}$$

where “cycl.” stands for contributions differing from the first term in the brackets by cyclic permutations of the momenta. For the counterterms we get from (3.23),

$$C_1(\mathbf{k}) = \delta^{(3)}(\mathbf{k}) \int [dq] I_2(\mathbf{q}, \mathbf{k}), \quad (\text{B.2a})$$

$$C_2(\mathbf{k}_1, \mathbf{k}_2) = \frac{1}{2} \delta^{(3)}(\mathbf{k}_1 + \mathbf{k}_2) \int [dq] \left(I_3(\mathbf{q}, \mathbf{k}_1, \mathbf{k}_2) - I_2(\mathbf{q}, \mathbf{k}_1 + \mathbf{k}_2) I_2(\mathbf{k}_1, \mathbf{k}_2) \right). \quad (\text{B.2b})$$

The last term in C_2 vanishes if the kernel I_2 satisfies

$$\lim_{p \rightarrow 0} I_2(\mathbf{q}, -\mathbf{q} + \mathbf{p}) I_2(\mathbf{k}, \mathbf{p}) = 0, \quad (\text{B.3})$$

which is indeed the case both for ZA and ED.

The 1-loop corrections to the Θ power spectrum are given by the diagrams shown in (3.30). The first — *daisy* — contribution reads,

$$\begin{aligned} P_{\text{daisy}}(\eta; |\mathbf{k}|) = & -e^{4\eta} \int [dq] \left[\left(I_2(-\mathbf{k}, \mathbf{k} - \mathbf{q}) I_2(-\mathbf{k}, \mathbf{q}) - \frac{1}{2} I_3(\mathbf{k}, -\mathbf{k}, \mathbf{q}) \right) \bar{P}(|\mathbf{k}|)^2 \right. \\ & \left. + \left(I_2(-\mathbf{q}, -\mathbf{k} + \mathbf{q}) I_2(\mathbf{k}, -\mathbf{q}) - \frac{1}{2} I_3(\mathbf{k}, \mathbf{q}, -\mathbf{q}) \right) \bar{P}(|\mathbf{q}|) \bar{P}(|\mathbf{k}|) + I_2^2(\mathbf{k}, -\mathbf{q}) \frac{\bar{P}(|\mathbf{q}|) \bar{P}(|\mathbf{k}|)^2}{\bar{P}(|\mathbf{k} - \mathbf{q}|)} \right]. \end{aligned} \quad (\text{B.4})$$

The second term, or *fish* diagram, gives,

$$\begin{aligned} P_{\text{fish}}(\eta; |\mathbf{k}|) = & e^{4\eta} \int [dq] \left[I_2(\mathbf{k}, -\mathbf{q}) I_2(\mathbf{k}, \mathbf{q} - \mathbf{k}) \bar{P}(|\mathbf{k}|)^2 + \frac{I_2(\mathbf{q}, \mathbf{k} - \mathbf{q})^2}{2} \bar{P}(|\mathbf{q}|) \bar{P}(|\mathbf{q} - \mathbf{k}|) \right. \\ & + I_2(\mathbf{k}, -\mathbf{q}) I_2(\mathbf{k} - \mathbf{q}, \mathbf{q}) \bar{P}(|\mathbf{q}|) \bar{P}(|\mathbf{k}|) + I_2(\mathbf{q} - \mathbf{k}, \mathbf{k}) I_2(\mathbf{k} - \mathbf{q}, \mathbf{q}) \bar{P}(|\mathbf{k} - \mathbf{q}|) \bar{P}(|\mathbf{k}|) \\ & \left. + \frac{I_2^2(\mathbf{q} - \mathbf{k}, \mathbf{k})}{2} \frac{\bar{P}(|\mathbf{q} - \mathbf{k}|) \bar{P}(|\mathbf{k}|)^2}{\bar{P}(|\mathbf{q}|)} + \frac{I_2^2(\mathbf{k}, -\mathbf{q})}{2} \frac{\bar{P}(|\mathbf{q}|) \bar{P}(|\mathbf{k}|)^2}{\bar{P}(|\mathbf{k} - \mathbf{q}|)} \right]. \end{aligned} \quad (\text{B.5})$$

Notice the presence of terms with the linear power spectrum $\bar{P}(|\mathbf{k}|)$ in the denominator. They arise as a result of the $1/\bar{P}$ dependence of the TSPT vertices. Such terms cannot appear in SPT, which is an analytic expansion in $\bar{P}(|\mathbf{k}|)$. Indeed, one verifies explicitly, that these terms cancel in the sum of (B.4) and (B.5). Another difference from SPT are the first terms in (B.4), (B.5) proportional to $\bar{P}(|\mathbf{k}|)^2$. They contain UV divergent momentum integrals which are independent of the power spectrum. The contributions with the kernels I_2 cancel between (B.4) and (B.5), whereas the contribution with I_3 is canceled by the third — *counterterm* — diagram from (3.30),

$$P_{\text{counter}} = -\frac{e^{4\eta}}{2} \bar{P}(|\mathbf{k}|)^2 \int [dq] I_3(\mathbf{k}, -\mathbf{k}, \mathbf{q}). \quad (\text{B.6})$$

The rest of terms are brought to the form,

$$\begin{aligned} P_{\Theta}^{1\text{-loop}}(\eta; |\mathbf{k}|) = & e^{4\eta} \int [dq] \left[\frac{1}{2} \bar{P}(|\mathbf{k}|) \bar{P}(|\mathbf{q}|) I_3(\mathbf{k}, \mathbf{q}, -\mathbf{q}) \right. \\ & \left. + \bar{P}(|\mathbf{k}|) \bar{P}(|\mathbf{k} - \mathbf{q}|) I_2(\mathbf{q} - \mathbf{k}, \mathbf{k}) I_2(\mathbf{k} - \mathbf{q}, \mathbf{q}) + \frac{I_2^2(\mathbf{q}, \mathbf{k} - \mathbf{q})}{2} \bar{P}(|\mathbf{q}|) \bar{P}(|\mathbf{k} - \mathbf{q}|) \right]. \end{aligned} \quad (\text{B.7})$$

Making use of eqs. (A.2), (A.3) one recovers the SPT result,

$$P_{\Theta\Theta}^{1-\text{loop}}(\eta; |\mathbf{k}|) = 2 \int [dq] \left[3G_3(\mathbf{k}, -\mathbf{q}, \mathbf{q}) P_\eta(|\mathbf{q}|) P_\eta(|\mathbf{k}|) + G_2^2(\mathbf{k} - \mathbf{q}, \mathbf{q}) P_\eta(|\mathbf{q}|) P_\eta(|\mathbf{k} - \mathbf{q}|) \right], \quad (\text{B.8})$$

where $P_\eta(|\mathbf{k}|)$ is the linear power spectrum at the time η .

To find the correction to the density power spectrum we need to add the three ‘composite operator’ diagrams (3.35). They read,

$$\hat{P}_{(i)}(\eta; |\mathbf{k}|) = e^{4\eta} \int [dq] \left[2I_2(\mathbf{k}, -\mathbf{q}) \bar{P}(|\mathbf{k}|) \bar{P}(|\mathbf{q}|) + I_2(\mathbf{q}, \mathbf{k} - \mathbf{q}) \bar{P}(|\mathbf{q}|) \bar{P}(|\mathbf{k} - \mathbf{q}|) \right] K_2(\mathbf{q}, \mathbf{k} - \mathbf{q}), \quad (\text{B.9a})$$

$$\hat{P}_{(ii)}(\eta; |\mathbf{k}|) = e^{4\eta} \int [dq] \frac{K_2(\mathbf{q}, \mathbf{k} - \mathbf{q})^2 \bar{P}(|\mathbf{k} - \mathbf{q}|) \bar{P}(|\mathbf{q}|)}{2}, \quad (\text{B.9b})$$

$$\hat{P}_{(iii)}(\eta; |\mathbf{k}|) = e^{4\eta} \int [dq] K_3(\mathbf{q}, -\mathbf{q}, \mathbf{k}) \bar{P}(|\mathbf{q}|) \bar{P}(|\mathbf{k}|). \quad (\text{B.9c})$$

Adding these contributions to $P_{\Theta\Theta}^{1-\text{loop}}$ and using (A.2), (A.3) we arrive at the SPT expression,

$$P_{\delta\delta}^{1-\text{loop}}(\eta; |\mathbf{k}|) = 6P_\eta(|\mathbf{k}|) \int [dq] F_3(\mathbf{k}, \mathbf{q}, -\mathbf{q}) P_\eta(|\mathbf{q}|) + 2 \int [dq] [F_2(\mathbf{q}, \mathbf{k} - \mathbf{q})]^2 P_\eta(|\mathbf{q}|) P_\eta(|\mathbf{k} - \mathbf{q}|). \quad (\text{B.10})$$

C IR safety and the initial power spectrum

The TSPT vertices $\bar{\Gamma}_n$ contain terms that have the initial power spectrum in the denominator and may, in principle, have IR divergence depending on its slope. Recall that these terms have to cancel in the final expressions for correlation functions. Thus, the IR singularities of Γ_n related to the slope of the power spectrum are spurious and cannot affect physical observables. We would like to mention that even in the presence of these singularities the statement of Sec. 5 that individual loop diagrams in TSPT are IR convergent if $\bar{P}(|\mathbf{q}|) \propto q^\nu$ with $\nu > -3$ at $q \rightarrow 0$ holds true, because Γ_n - vertices have to be multiplied by loop propagators inside loops so that eventually the singular contributions are completely cancelled.

The 2-point vertex $\bar{\Gamma}'_2(-\mathbf{q}, \mathbf{q})$ is finite provided that the initial power spectrum does not vanish anywhere. In the real universe, however, $\bar{P}(|\mathbf{q}|) \propto q$ at $q \rightarrow 0$ and thus, formally $\bar{\Gamma}'_2 \sim 1/q$ in the soft limit. We will now show that the divergence related to the $1/P$ terms are absent in higher order vertices if at least two of their arguments are hard¹⁷ and the power spectrum behaves as $\bar{P}(|\mathbf{q}|) \propto q^\nu$ with $\nu \leq 2$ at $q \rightarrow 0$. This includes the case of the real universe where $\nu = 1$.

¹⁷A configuration with a single hard momentum is forbidden by the momentum conservation.

Let us start with the $\bar{\Gamma}_3$ vertex in the limit where two momenta, \mathbf{k} , $(-\mathbf{k}-\mathbf{q})$, are hard and the third one is soft, $\mathbf{q} \equiv \epsilon \mathbf{q}'$, $\epsilon \rightarrow 0$. We use the expression (4.9b) and focus on the term $\sim 1/\bar{P}(|\mathbf{q}|)$ (the IR divergences cancel for other terms, see Sec. 5),

$$\bar{\Gamma}'_3(-\mathbf{k}-\mathbf{q}, \mathbf{k}, \mathbf{q}) \ni \frac{I_2(-\mathbf{k}-\mathbf{q}, \mathbf{k})}{\bar{P}(|\mathbf{q}|)} \propto \frac{q^2}{k^2} \frac{1}{\bar{P}(|\mathbf{q}|)}. \quad (\text{C.1})$$

We see that there is no IR divergence provided that $\bar{P}(|\mathbf{q}|) \propto q^\nu$ with $\nu \leq 2$ at $q \rightarrow 0$. This result can be readily generalized to an arbitrary vertex with a number of soft and hard momenta. Let us prove it by induction in the case of two hard momenta and all other momenta uniformly sent to zero as in (5.1). As an induction hypothesis we assume that the terms $\sim 1/\bar{P}(|\mathbf{q}_i|)$ entering the vertex $\bar{\Gamma}'_{n-1}(\mathbf{k}, -\mathbf{k}-\sum_{i=1}^{n-3} \mathbf{q}_i, \mathbf{q}_1, \dots, \mathbf{q}_{n-3})$ scale as $\epsilon^2/P(\epsilon|\mathbf{q}'|) \sim \epsilon^2/P(\epsilon)$. We will use the shorthand $\mathbf{q} \equiv \sum_{i=1}^{n-2} \mathbf{q}_i$. It is convenient to divide the vertex Γ'_n into two pieces,

$$\bar{\Gamma}'_n = -\frac{1}{n-2} (\bar{\Gamma}'_{n,A} + \bar{\Gamma}'_{n,B}), \quad (\text{C.2})$$

where $\bar{\Gamma}'_{n,A}$ is the piece of the recursion relations (4.12), (4.3) common in ZA and ED, and $\bar{\Gamma}'_{n,B}$ is a contribution appearing in ED (second line of (4.12)). One has,

$$\bar{\Gamma}'_{n,A}(\mathbf{k}, -\mathbf{k}-\mathbf{q}, \mathbf{q}_1, \dots, \mathbf{q}_{n-2}) = \sum_{j=1}^{n-2} I_2(\mathbf{q}_j, \mathbf{k}) \bar{\Gamma}'_{n-1}(\mathbf{k} + \mathbf{q}_j, \dots, \check{\mathbf{q}}_j, \dots) \quad (\text{C.3a})$$

$$+ \sum_{j=1}^{n-2} I_2(\mathbf{q}_j, -\mathbf{k}-\mathbf{q}) \bar{\Gamma}'_{n-1}(\mathbf{k}, -\mathbf{k}-\mathbf{q} + \mathbf{q}_j, \dots, \check{\mathbf{q}}_j, \dots) \quad (\text{C.3b})$$

$$+ \sum_{l>j=1}^{n-2} I_2(\mathbf{q}_j, \mathbf{q}_l) \bar{\Gamma}'_{n-1}(\dots, \mathbf{q}_j + \mathbf{q}_l, \dots, \check{\mathbf{q}}_l, \dots) \quad (\text{C.3c})$$

$$+ I_2(\mathbf{k}, -\mathbf{k}-\mathbf{q}) \bar{\Gamma}'_{n-1}(-\mathbf{q}, \mathbf{q}_1, \dots, \mathbf{q}_{n-2}). \quad (\text{C.3d})$$

As was proven in Sec. 5, the IR divergences appearing in the first two terms (C.3a), (C.3b) cancel up to $O(\epsilon^0)$ order. According to the induction hypothesis the corresponding vertices already contain the terms $\sim \epsilon^2/\bar{P}(\epsilon)$ and thus satisfy the hypothesis. The term (C.3c) diverges only as $\sim \epsilon^2/\bar{P}(\epsilon)$ because $I_2(\mathbf{q}_i, \mathbf{q}_j) \sim O(\epsilon^0)$. Finally, the term (C.3d) features the vertex scaling as $1/\bar{P}(\epsilon)$ that multiplies the following I_2 kernel,

$$I_2(\mathbf{k}, -\mathbf{k}-\mathbf{q}) = O(q^2/k^2) = O(\epsilon^2). \quad (\text{C.4})$$

Thus, we have checked that the $\bar{\Gamma}'_{n,A}$ piece satisfies the induction hypothesis. Now we turn to the case of $\bar{\Gamma}'_{n,B}$. This contribution contains the K_n kernels which were proven to be at least $O(\epsilon^0)$ for any momenta configuration (see (5.2)). Thus, if one of those multiplies the $\bar{\Gamma}'_n(\mathbf{k}, -\mathbf{k}, \dots)$ vertex, it will not produce any IR enhancement. The only term that does

not obviously satisfy the induction hypothesis is

$$\begin{aligned} \bar{\Gamma}_{n,B}(\mathbf{k}, -\mathbf{k} - \mathbf{q}, \mathbf{q}_1, \dots, \mathbf{q}_{n-2}) \ni \\ \frac{3}{2} \sum_{m=3}^{n-1} \frac{1}{(m-2)!(n-m)!} \sum_{\sigma} K_m(\mathbf{k}, -\mathbf{k} - \mathbf{q}, \mathbf{q}_{\sigma(1)}, \dots, \mathbf{q}_{\sigma(m-2)}) \\ \times \bar{\Gamma}'_{n-m+1}(-\sum_{l=m-2}^{n-2} \mathbf{q}_{\sigma(l)}, \mathbf{q}_{\sigma(m-2)}, \dots, \mathbf{q}_{\sigma(n-2)}) \end{aligned} \quad (\text{C.5a})$$

In order to show that this term scales as $\epsilon^2/P(\epsilon)$ it is sufficient to prove that the K_m kernels go as $\sim \epsilon^2$ in the limit where two hard momenta almost satisfy momentum conservation,

$$\lim_{\epsilon \rightarrow 0} K_m(\mathbf{k}, -\mathbf{k} - \epsilon \mathbf{q}', \epsilon \mathbf{q}'_1, \dots, \epsilon \mathbf{q}'_{m-2}) = O(\epsilon^2), \quad m \geq 3. \quad (\text{C.6})$$

This behavior is obviously satisfied for $m = 2$, see (4.11b). Suppose now the above is true for some $m - 1$. Recall that in Sec. 5.1 we have proven that the kernels K_n are bounded for *all* values of momenta. Then using (4.11c) one can readily see that most of the terms in the recursion relation satisfy the induction hypothesis because the corresponding kernels have the same momenta configuration as (C.6) and multiply some other $O(\epsilon^0)$ terms. The rest is given by

$$\begin{aligned} \frac{(2n+3)}{2} K_m(\mathbf{k}, -\mathbf{k} - \mathbf{q}, \mathbf{q}_1, \dots, \mathbf{q}_{m-2}) \ni \\ \alpha(\mathbf{k}, -\mathbf{k} - \mathbf{q} + \tilde{\mathbf{q}}) K_{m-1}(-\mathbf{k} - \mathbf{q}, \mathbf{q}_1, \dots) + \alpha(-\mathbf{k} - \mathbf{q}, \mathbf{k} + \tilde{\mathbf{q}}) K_{m-1}(\mathbf{k}, \mathbf{q}_1, \dots) \end{aligned} \quad (\text{C.7a})$$

$$- \sum_{i=1}^{m-2} I_2(\mathbf{k}, \mathbf{q}_i) K_{m-1}(\mathbf{k} + \mathbf{q}_i, -\mathbf{k} - \mathbf{q}, \check{\mathbf{q}}_j) - \sum_{i=1}^{m-2} I_2(-\mathbf{k}, \mathbf{q}_i) K_{m-1}(-\mathbf{k} - \mathbf{q} + \mathbf{q}_i, \mathbf{k}, \check{\mathbf{q}}_j), \quad (\text{C.7b})$$

where $\tilde{\mathbf{q}} \equiv \sum_{i=1}^{m-2} \mathbf{q}_i$. One can show that the sum of the terms (C.7a) is $O(\epsilon^2)$ as a consequence of¹⁸

$$K_m(\mathbf{k}, \mathbf{q}_1, \dots, \mathbf{q}_{m-1}) = K_m(-\mathbf{k}, \mathbf{q}_1, \dots, \mathbf{q}_{m-1}) + O(\epsilon). \quad (\text{C.8})$$

Finally, in (C.7b) the pole contributions from the I_2 kernel cancel up to $O(\epsilon^0)$ so that the residual term remains $O(\epsilon^2)$ because of the induction hypothesis. This completes the proof for the case of two hard momenta. Extension to the case of more hard momenta is straightforward.

In summary, we have shown that the $\bar{\Gamma}'_n$ vertices with at least some of their arguments hard do not contain any divergences in the IR limit provided that $\bar{P}(k) \propto k^\nu$, $\nu \leq 2$ at $k \rightarrow 0$, which is the case for realistic cosmology.

¹⁸This property can be straightforwardly proven by induction. Indeed, if one assumes Eq.(C.8) is true for all $l \leq m - 1$, one can write down the recursion relation (4.11c) that generates $K_m(\mathbf{k}, \mathbf{q}_1, \dots)$. Then one can notice that after the cancellation of IR dangerous contributions (see Eq.(5.2)) the remainders of the corresponding α and β kernels are even functions of \mathbf{k} at order $O(\epsilon^0)$, and thus, to this order, one can safely substitute all $K_l(\mathbf{k}, \mathbf{q}_1, \dots) (l \leq m - 1)$ with $K_l(-\mathbf{k}, \mathbf{q}_1, \dots)$ in the recursion relation, which will immediately yield (C.8).

References

- [1] P.J.E. Peebles, *The Large-scale Structure of the Universe*, Princeton University Press (1980).
- [2] S. Pueblas and R. Scoccimarro, Phys. Rev. D **80** (2009) 043504 [arXiv:0809.4606 [astro-ph]].
- [3] D. Baumann, A. Nicolis, L. Senatore and M. Zaldarriaga, JCAP **1207**, 051 (2012) [arXiv:1004.2488 [astro-ph.CO]].
- [4] M. Pietroni, G. Mangano, N. Saviano and M. Viel, JCAP **1201** (2012) 019 [arXiv:1108.5203 [astro-ph.CO]].
- [5] J. J. M. Carrasco, M. P. Hertzberg and L. Senatore, JHEP **1209**, 082 (2012) [arXiv:1206.2926 [astro-ph.CO]].
- [6] T. Baldauf, E. Schaan and M. Zaldarriaga, “On the reach of perturbative descriptions for dark matter displacement fields,” arXiv:1505.07098 [astro-ph.CO].
- [7] F. Bernardeau, S. Colombi, E. Gaztanaga and R. Scoccimarro, Phys. Rept. **367** (2002) 1 [astro-ph/0112551].
- [8] F. Bernardeau, “The evolution of the large-scale structure of the universe: beyond the linear regime,” arXiv:1311.2724 [astro-ph.CO].
- [9] P. A. R. Ade *et al.* [Planck Collaboration], “Planck 2015 results. XVII. Constraints on primordial non-Gaussianity,” arXiv:1502.01592 [astro-ph.CO].
- [10] M. H. Goroff, B. Grinstein, S. J. Rey and M. B. Wise, Astrophys. J. **311** (1986) 6.
- [11] E. T. Vishniac, MNRAS **203**, 345 (1983).
- [12] B. Jain and E. Bertschinger, Astrophys. J. **456** (1996) 43 [astro-ph/9503025].
- [13] R. Scoccimarro and J. Frieman, Astrophys. J. Suppl. **105**, 37 (1996) [astro-ph/9509047].
- [14] P. Creminelli, J. Noreña, M. Simonović and F. Vernizzi, JCAP **1312**, 025 (2013) [arXiv:1309.3557 [astro-ph.CO]].
- [15] D. Blas, M. Garny and T. Konstandin, JCAP **1309**, 024 (2013) [arXiv:1304.1546 [astro-ph.CO]].
- [16] J. J. M. Carrasco, S. Foreman, D. Green and L. Senatore, JCAP **1407** (2014) 056 [arXiv:1304.4946 [astro-ph.CO]].
- [17] N. S. Sugiyama and D. N. Spergel, JCAP **1402** (2014) 042 [arXiv:1306.6660 [astro-ph.CO]].
- [18] A. Kehagias and A. Riotto, Nucl. Phys. B **873** (2013) 514 [arXiv:1302.0130 [astro-ph.CO]].
- [19] M. Peloso and M. Pietroni, JCAP **1305** (2013) 031 [arXiv:1302.0223 [astro-ph.CO]].
- [20] D. Blas, M. Garny and T. Konstandin, JCAP **1401**, 010 (2014) [arXiv:1309.3308].
- [21] D. J. Eisenstein, H. j. Seo and M. J. White, Astrophys. J. **664** (2007) 660 [astro-ph/0604361].
- [22] M. Crocce and R. Scoccimarro, Phys. Rev. D **77** (2008) 023533 [arXiv:0704.2783 [astro-ph]].
- [23] L. Senatore and M. Zaldarriaga, JCAP **1502**, 013 (2015) [arXiv:1404.5954 [astro-ph.CO]].
- [24] T. Baldauf, M. Mirbabayi, M. Simonović and M. Zaldarriaga, Phys. Rev. D **92**, no. 4, 043514 (2015) [arXiv:1504.04366 [astro-ph.CO]].
- [25] S. Foreman, H. Perrier and L. Senatore, “Precision Comparison of the Power Spectrum in the EFTofLSS with Simulations,” arXiv:1507.05326 [astro-ph.CO].

- [26] T. Baldauf, L. Mercolli and M. Zaldarriaga, “The Effective Field Theory of Large Scale Structure at Two Loops: the apparent scale dependence of the speed of sound,” arXiv:1507.02256 [astro-ph.CO].
- [27] A. A. Abolhasani, M. Mirbabayi and E. Pajer, “Systematic Renormalization of the Effective Theory of Large Scale Structure,” arXiv:1509.07886 [hep-th].
- [28] T. Nishimichi, F. Bernardeau and A. Taruya, “Anomalous coupling of the small-scale structures to the large-scale gravitational growth,” arXiv:1411.2970 [astro-ph.CO].
- [29] M. Garny, T. Konstandin, R. A. Porto and L. Sagunski, JCAP **1511**, 032 (2015) [arXiv:1508.06306 [astro-ph.CO]].
- [30] D. Blas, S. Floerchinger, M. Garny, N. Tetradis and U. A. Wiedemann, JCAP **1511**, 049 (2015) [arXiv:1507.06665 [astro-ph.CO]].
- [31] F. F hrer and G. Rigopoulos, “On Renormalizing Viscous Fluids as Models for Large Scale Structure Formation,” arXiv:1509.03073 [astro-ph.CO].
- [32] D. Blas, M. Garny, M. M. Ivanov and S. Sibiryakov, “Time-Sliced Perturbation Theory II: Baryon Acoustic Oscillations and Infrared Resummation,” arXiv:1605.02149 [astro-ph.CO].
- [33] M. Pietroni, JCAP **0810**, 036 (2008) [arXiv:0806.0971 [astro-ph]].
- [34] P. Valageas, Astron. Astrophys. **421**, 23 (2004) [astro-ph/0307008].
- [35] S. M. Carroll, S. Leichenauer and J. Pollack, Phys. Rev. D **90** (2014) 023518 [arXiv:1310.2920 [hep-th]].
- [36] B. Audren and J. Lesgourgues, JCAP **1110** (2011) 037 [arXiv:1106.2607 [astro-ph.CO]].
- [37] S. Tassev and M. Zaldarriaga, JCAP **1204** (2012) 013 [arXiv:1109.4939 [astro-ph.CO]].
- [38] B. Horn, L. Hui and X. Xiao, JCAP **1409** (2014) 09, 044 [arXiv:1406.0842 [hep-th]].
- [39] W. D. Goldberger, L. Hui and A. Nicolis, Phys. Rev. D **87** (2013) 10, 103520 [arXiv:1303.1193 [hep-th]].